Doctor Thesis

桿体と錐体における視物質リン酸化とその制御機構

Sensory Transduction Group (Prof. Kawamura)
Nanobiology Laboratories
Graduate School of Frontier Biosciences
Osaka University

Daisuke Arinobu

March 2010

Summary

In the vertebrate retina, there are two types of photoreceptors, rods and cones. Rods mediate twilight vision and cones mediate daylight vision. Although both rods and cones respond to light by evoking light responses, they are different in their response properties. Previous study showed that visual pigment phosphorylation, a quenching mechanism of light-activated visual pigment, is much more rapid in cones than in rods. In the present study, I measured the early time course of this rapid phosphorylation with high time resolution and directly compared it with the photoresponse time course in cones obtained under similar light conditions as those used for the phosphorylation measurement. In this comparison, at the time of photoresponse recovery, almost two phosphates were incorporated into a bleached cone pigment, which indicated that the visual pigment phosphorylation coincides with the photoresponse recovery. Because the activity of visual pigment kinase in cones is very high, cone pigment is readily phosphorylated at very high bleach levels, which probably explains why cone photoresponses recover quickly even after a very bright light and do not saturate under intense background light.

Visual pigment kinase, GRK1 in rods and GRK7 in cones, is regulated by a neuronal calcium sensor protein (NCS), S-modulin in rods and visinin in cones, in the carp retina. I compared Ca^{2+}-dependent regulation of GRK1 by S-modulin and that of GRK7 by visinin. I first measured the expression levels of S-modulin and visinin, and estimated their concentrations in the outer segment. The result showed that visinin in cones was 20 times more abundant than S-modulin in rods. I also compared the dose-dependency and the Ca^{2+}-dependency of the inhibitory effect of S-modulin on GRK1 in rods and that of visinin on GRK7 in cones. Based on these measurements I estimated the inhibition of GRK in intact cells: the inhibition of GRK7 by visinin would be 2.5 times higher in cones than in rods at the Ca^{2+} concentration in the dark. Because the inhibition is lost under bright light, this larger inhibitory effect in cones would expand the range of Ca^{2+}-dependent regulation on GRK7 activity in cones. I also measured the dose-dependent and Ca^{2+}-dependent inhibitions on GRK7 (cone GRK) by S-modulin (rod NCS) and those on GRK1 (rod GRK) by visinin (cone NCS). Although S-modulin and visinin are expressed in a cell-type specific manner, I could not observe a significant difference in their inhibitory activities. This finding could indicate that cell-type specific

expression of a protein does not always mean that the protein has a cell-type specific effect. S-modulin and visinin may have cell-type specific roles in the regulation of reactions other than visual pigment phosphorylation. A GRK7 peptide of the N-terminus region, the binding domain of GRK to photoreceptor NCS, showed slightly higher affinity to S-modulin and visinin than the corresponding GRK1 peptide. The higher affinity of N-terminal region of GRK7 to S-modulin and visinin could cause the higher inhibition of GRK7 by S-modulin and visinin.

General introduction

We can see the external world under light conditions that range from dim to bright light, where the difference of light intensity is almost a thousand-million-fold. Our eyes have an ability to detect light signals of various intensities. For this ability, in the vertebrate retina, there are two types of photoreceptor cells, rods and cones (Figure 1A). Although both types of the cells convert light signals to neural signals, their characteristics of the photoresponse are different (Nakatani and Yau, 1989; Perry and McNaughton, 1991; Miller and Korenbrot, 1993; Burkhardt, 1994). The light sensitivity of a rod is 10^2-10^3 times higher than that of a cone (Figure1C). Because of the high

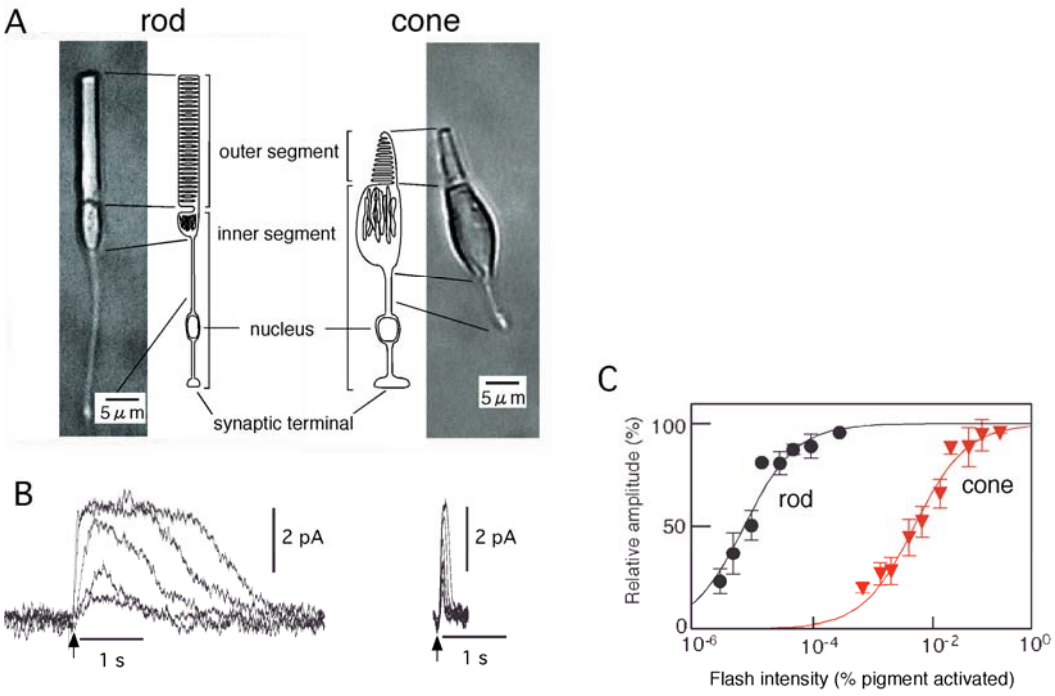

Figure 1. Characteristics of rods and cones. (A) A rod and a cone brushed off the carp retina. The sketch shows the structure of each cell. Both cells consist of two parts, the outer segment (OS) and the inner segment (IS). (B) Families of photoresponses of a rod (left) and a red-sensitive cone (right) obtained by giving light flashes of various intensities. Arrows indicate the timing of the delivery of a light flash. (C) Flash intensity-response relations of rods and red-sensitive cones. (B and C), modified from Fig. 1 in Tachibanaki *et al*. (2001).

light-sensitivity of a rod, rods mediate twilight vision. The time course of a rod flash response is slow (Figure 1B). The recovery of a response delays significantly after termination of a light stimulus, and because of this characteristics, in the twilight, it is no easy to detect an object moving quickly. Cones are less sensitive to light (Figure 1C) and mediate daylight vision. Cones respond to on and off of a light stimulus without significant delays (Figure 1B). This characteristic contributes to the improved time resolution in the detection of light in cones over rods. Thus, the motion detection is easier in cones than in rods.

The phototransduction cascade to generate a photoresponse in rods is well understood (Figure 2) (Burns and Arshavsky, 2005; Lamb and Pugh, 2006; Fu and Yau, 2007). In rods, a photon activates a visual pigment molecule. The activated visual pigment activates a GTP-binding protein, transducin, by substitution of GTP for GDP. Activated transducin activates cGMP phosphodiesterase (PDE) that hydrolyzes cGMP. As a result, cGMP concentration is decreased in the light. The

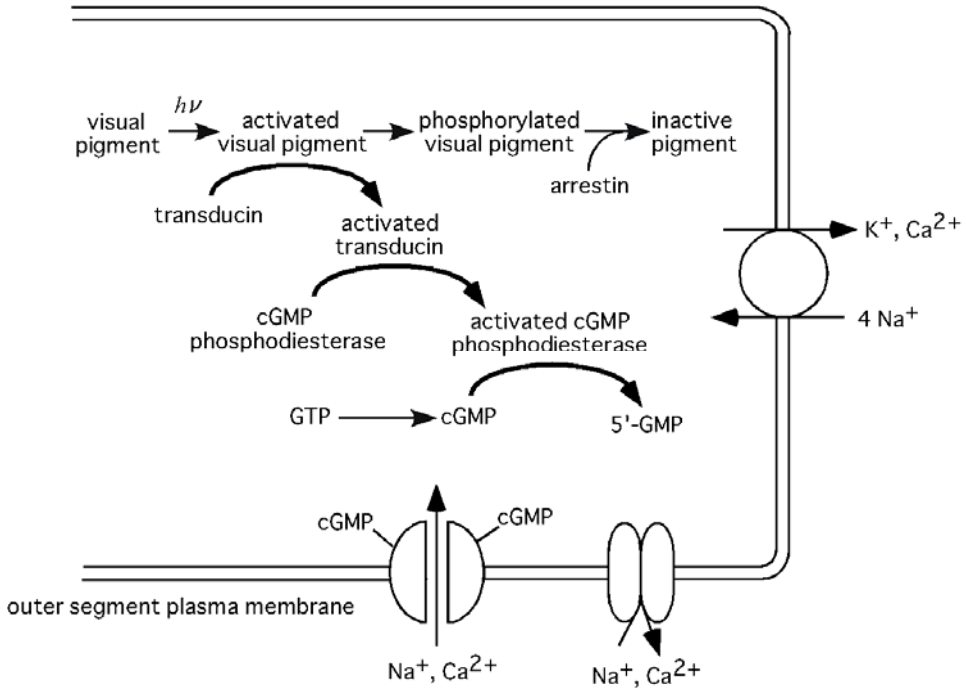

Figure 2. Phototransduction cascade in vertebrate rods and cones. In the outer segment of a rod and a cone, cGMP concentration decreased by light stimulation through this cascade (see details in text). Modified from Fig.2 in Kawamura and Tachibanaki (2008).

decrease in the cGMP concentration causes closure of a cGMP-gated cation channel present in the plasma membrane of the outer segment (OS), and therefore induces a hyperpolarizing light response. The closure of the cGMP-gated channel blocks the entry of Ca^{2+} that flows into the OS through this channel in the dark. In the plasma membrane of the OS, a Na^{+}/Ca^{2+}-K^{+} exchanger continuously extrudes Ca^{2+} from the inside of the OS. As a consequence, cytoplasmic Ca^{2+} concentration decreases during a light response (Pugh and Lamb, 2000; Fain *et al.*, 2001; Burns and Arshavsky, 2005). This decrease is detected by Ca^{2+}-binding proteins such as S-modulin and guanylate cyclase activating protein (GCAP), and these proteins affect the hydrolysis and the synthesis of cGMP, respectively. It has been known that the decrease in the Ca^{2+} concentration in the light is the key event of light-adaptation. Especially, GCAP has been to shown to be essential for the decrease in the light-sensitivity during light-adaptation. GCAP is known to be in an active form at low Ca^{2+} concentrations, and therefore, in the light. The increased synthesis of cGMP in the light is expected to increase the number of the channels open to allow the increase in the inward current. As a result, we can expect that the light response becomes small as the light stimulus continues, which is exactly the consequence of light-adaptation.

It has been known that there are rod and cone versions of phototransduction enzymes. From this result, the phototransduction cascades in rods and cones are thought to be basically similar. It is therefore possible that the differences in photoresponse properties between rods and cones are because of differences in the phototransduction reactions in rods and cones. As shown in Figure 1B, termination of light response is very rapid in cones. In the present study, I focused on this quick termination of light response in cones. Especially, I concentrated on the phosphorylation of activated visual pigment that is the first reaction responsible for the termination of the phototransduction cascade.

Part 1. Measurement of visual pigment phosphorylation time course

Introduction

To shut off a light response, the activated species of each player in the phototransduction cascade must be inactivated at the cessation of light. The activated visual pigment is inactivated first by phosphorylation of activated visual pigment by a G-protein coupled receptor kinase (GRK; GRK1 in rods). Arrestin then binds to the phosphorylated visual pigment to completely shut off its activity (Maeda *et al.*, 2003). In cones, a distinct visual pigment kinase (GRK7) has been reported in some classes of vertebrate, including teleosts (Hisatomi *et al.*, 1998; Weiss *et al.*, 1998; Weiss *et al.*, 2001). In the study by Tachibanaki *et al.* (2001), visual pigment phosphorylation was at least 20 times faster in cones than in rods and completed within 1 sec after light flash in a membrane preparation of purified carp cones (Figure 3). Similar rapid phosphorylation in blue cones was observed in a living zebrafish (Kennedy *et al.*, 2004). This rapid phosphorylation is probably one of the underlying mechanisms of quick termination of a cone photoresponse. However, because the

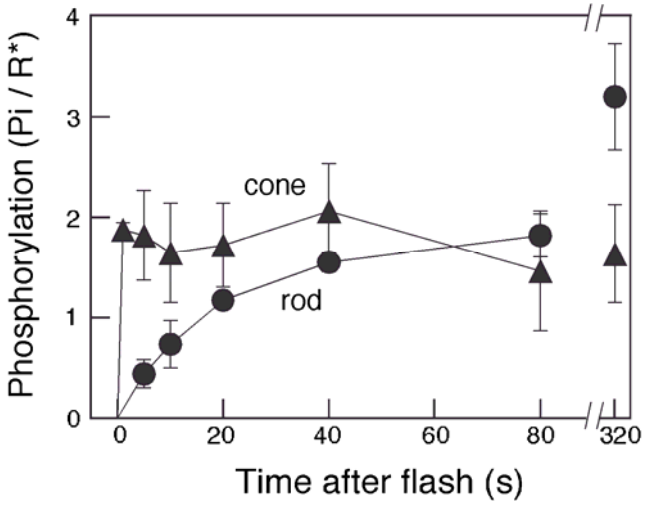

Figure 3. Time course of visual pigment phosphorylation in rod and the cone membranes. ^{32}P incorporated into the visual pigment was quantified in rod and cone membranes. The bleach level was 1.9 % in the rod membranes and 4 % in the cone membranes. Modified from Fig. 3 in Tachibanaki *et al.* (2001).

reaction was too rapid, the early phase of the phosphorylation reaction could not be measured precisely in these studies. In this study, I tried to measure the rapid phosphorylation time course in the cone membranes by using a rapid-quench apparatus.

Experimental Procedures

Preparation of rod and cone membranes

Carp (*Cyprinus carpio*) rods and cones were isolated in a carp Ringer's solution (119.9 mM NaCl, 2.6 mM KCl, 0.5 mM $CaCl_2$, 0.5 mM $MgCl_2$, 0.5 mM $MgSO_4$, 1 mM $NaHCO_3$, 16 mM glucose, 0.5 mM NaH_2PO_4, 4 mM HEPES, pH 7.5), and purified by centrifugation with using a stepwise Percoll density gradient consisted of 30/45/60/70/75/90% (w/v) Percoll (Tachibanaki *et al.*, 2005). Purified rods and cones were washed additionally with a potassium gluconate buffer 1 (K-gluc buffer 1; 115 mM potassium gluconate, 2.5 mM KCl, 3 mM $MgCl_2$, 0.2 mM EGTA, 0.1 mM $CaCl_2$, 10 mM HEPES, 1 mM dithiothreitol, pH 7.5) by centrifugation (600 × g for 12 sec and then 3,000 × g for 4 sec). The resultant purified rods and cones were frozen, freeze-thawed and washed twice with a K-gluc buffer 1. An aliquot of the washed membranes was used to quantify the amount of visual pigment in the rod and the cone membranes. The washed membranes were stored in the dark at -80°C until use.

Phosphorylation assays

Phosphorylation assay was performed as described (Tachibanaki *et al.*, 2005). Rod or cone membranes (15 μl) were mixed with 10 μl of the K-gluc buffer 1 containing [γ-^{32}P] ATP, GTP, and EGTA. The ATP concentration used was 1 mM in the measurements in the cone membranes, and it was either 1 mM or 100 μM in the measurements in the rod membranes. After preincubation for 30 sec, the sample was irradiated with a light flash. The bleach level of the visual pigments was 1.3% and 75% in rod membranes, and 2.5%, 23%, 54% and 95% in cone membranes. The reaction was terminated by adding 150 μL of 10% (w/v) trichloroacetic acid. After centrifugation (20,000 × g for 10 min), the precipitate was washed with K-gluc buffer 1 and subjected to SDS-PAGE, and the amount of ^{32}P incorporated into the visual pigment band was quantified by using an image analyzer (BAS 2500; Fuji Film, Tokyo, Japan). Dark activities, which were almost negligible, were always subtracted to determine the light-dependent incorporation of ^{32}P. Phosphorylation of visual pigment is expressed in units of the number of phosphates incorporated per visual pigment bleached (Pi/R*) or total amount of phosphate (pmol of Pi).

Results

Visual pigment phosphorylation in rods and cones

Visual pigment activated by light is inactivated by the phosphorylation. To compare the time course of visual pigment phosphorylation between rods and cones, I first purified rods and cones from the carp retina (see Experimental Procedures). Briefly, rods and cones were brushed off the retina (Figure 4A). The cells were purified by using a stepwise Percoll density gradient. Rods were collected at the 45/60% (w/v) interface (Figure 4B), and cones were collected at the 75/90% (w/v) interface (Figure 4C).

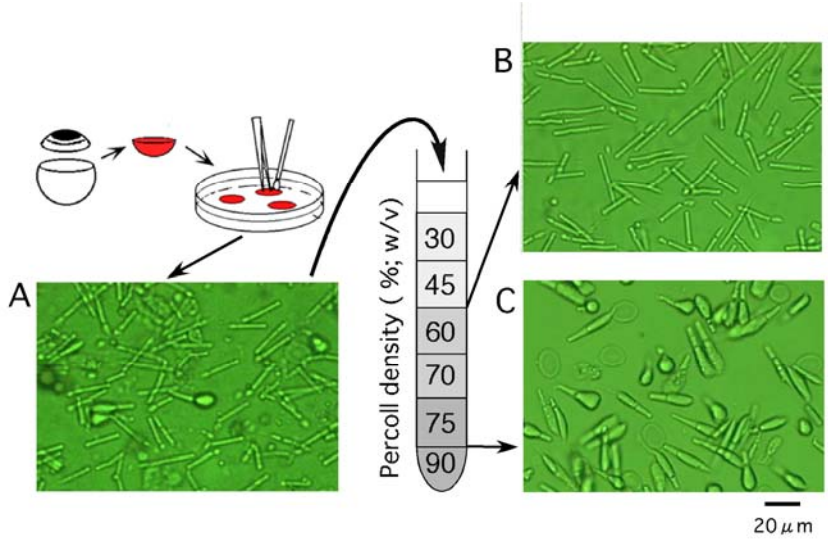

Figure 4. Purification of rods and cones from carp retina. Photoreceptor cells were brushed off the retina (A). The mixture of rods and cones was layered on the top of a Percoll stepwise density gradient. After centrifugation, rods were obtained at the 45/60% interface (B), and cones were obtained at the 75/90% interface (C). Modified from Fig. 1 in Tachibanaki *et al.* (2001).

In cones, the time course of visual pigment phosphorylation was measured previously (Figure 3, Tachibanaki *et al.*, 2001). However, the time course of the phosphorylation was too fast to measure with manual operation used in that study. Thus, a rapid-quench apparatus shown in Figure 5A was constructed and visual pigment phosphorylation was measured by using this apparatus.

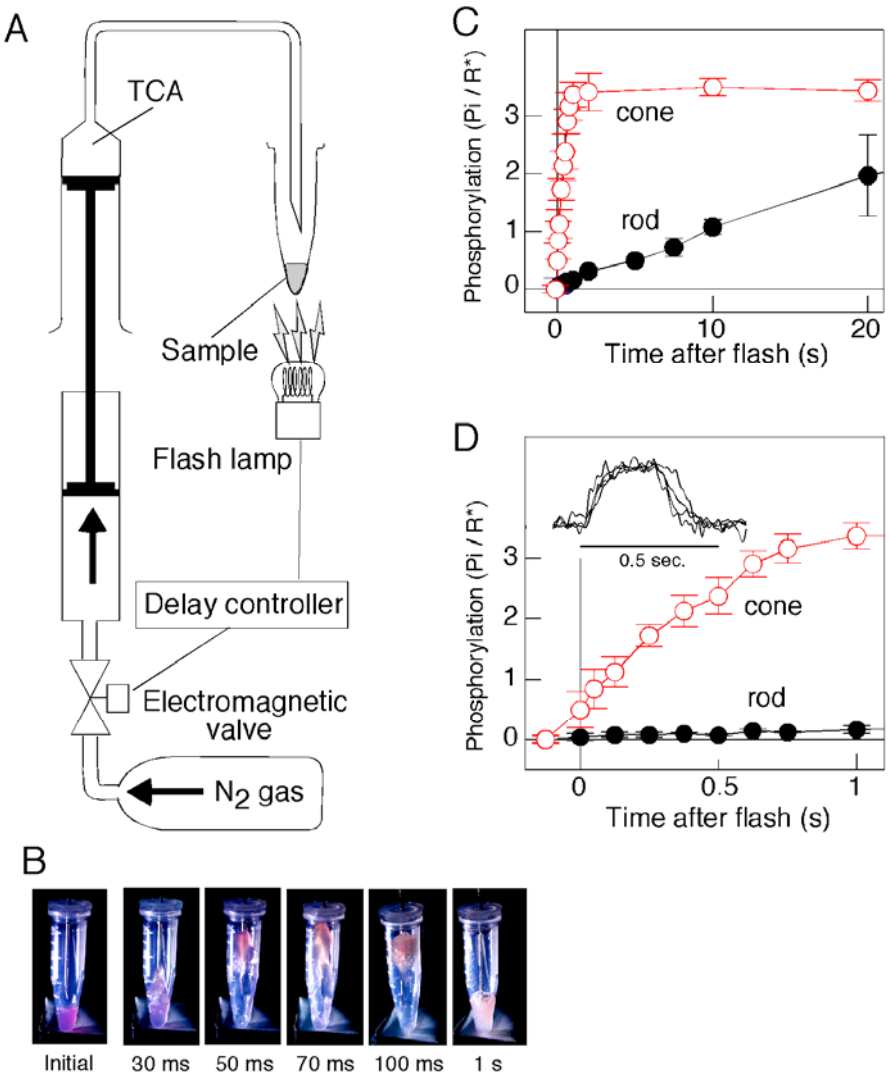

Figure 5. Comparison of the rate of visual pigment phosphorylation between rods and cones.

(A) Schematic drawing of the rapid-quench apparatus (see text for details). (B) The color changes of rhodopsin (from purple to orange) are the result of denaturation after adding TCA. Protein denaturation was found to be completed 50-70 ms after the addition of TCA. (C) Phosphorylation time course in rod (filled circles) and cone (open circles) membranes using the rapid-quench apparatus (n = 3). The bleach level was 1.3% in the rod membranes and 2.5% in the cone membranes. (D) Same phosphorylation time course as in C at an expanded time scale. (*Inset*) Normalized carp red-sensitive cone photoresponses (n = 4) elicited by a light flash of which intensity was similar to that used in the phosphorylation measurement (2.3% of the red pigment bleached).

Phosphorylation reactions were initiated by a light flash to the sample in a test tube, and were terminated by adding trichloroacetic acid (TCA). The timing of the addition of TCA after a light flash was controlled by a computer that opens an electric valve to supply a nitrogen gas pressure (5 kg/cm^2) to a syringe containing TCA. It takes 30 ms for the actual TCA delivery to the sample from the opening of the valve. The delay was subtracted in data analysis. The time necessary to quench the reaction after adding TCA was calibrated by observing color changes accompanied by denaturation of rhodopsin (Figure 5B). TCA was added to a suspension of rod membranes at time 0 in the dark, and a photograph was taken by giving a light flash at various time intervals after adding TCA. By visual observation of the color change from purple to orange, denaturation of rhodopsin by TCA was found to be completed 50-70 ms after adding TCA. This delay was not subtracted in data analysis because of relative uncertainty of the time required for the color change.

Figure 5C shows the phosphorylation time course in rod and cone membranes at a slow time scale, and Figure 5D shows the same at an expanded time scale. As seen, cone visual pigment phosphorylation (open circles) is very rapid. The initial phosphorylation rate was 0.09 Pi incorporated into an activated visual pigment per second (Pi/R*/sec) in rods and 4.8 Pi/R*/sec in cones. The phosphorylation rate was 50 times faster in cones. In Figure 5D, inset shows the carp red-sensitive cone photoresponses elicited by a light flash of similar light intensity (2.3 % pigment bleach) used in the phosphorylation measurement (2.5 % pigment bleach) in Figure 5. The photoresponses started to recover at 0.3 s after the light flash. At the time of this recovery, about two phosphates were incorporated into an activated cone visual pigment.

Visual pigment phosphorylation at high bleach levels

It has been well known that rod responses remain saturated for >10 sec when the light stimulus is intense (Pepperberg *et al.*, 1992), whereas cone responses recover rather quickly even after exposure to very bright light (Normann and Werblin, 1974; Burkhardt, 1994) (see Figure 6B and C insets). As shown in Figure 5, the cone kinase activity is very high so that cone kinase may be able to phosphorylate cone pigment even at very high bleach levels enough to recover photoresponse. In Figure 6A, I measured the time course of rod and cone visual pigment phosphorylation at various bleach levels in rod membranes and cone membranes. In Figure 6A, the total phosphorylation is

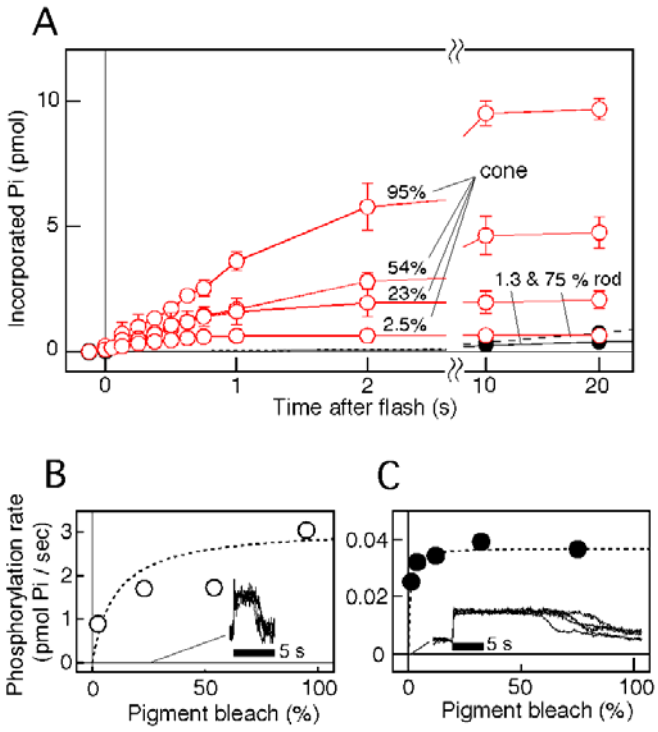

Figure 6. Visual pigment phosphorylation at high bleach levels. (A) Phosphorylation time courses at high bleach levels in rod and cone membranes. Phosphorylation time courses were measured at indicated bleach levels in rod and cone membranes containing 7.5 pmol of visual pigment (n = 3 in both membranes). (B and C) Initial phosphorylation rates determined in A were plotted as a function of bleach level for the cone (B) and rod (C) membranes. (*Insets*) The normalized photoresponses elicited by bright light flash (28% bleach) in carp red cones (four cells, B) and a bright light flash (0.3% bleach) in frog rods (five cells, C). The dotted curves were drawn based on a Michaelis-Menten equation, $V = V_{max} S / (S + K_m)$, with K_m = 10% bleach and V_{max} = 3.1 Pi / sec for the cone membranes (B), and with K_m = 0.61% bleach and V_{max} = 0.037 Pi / sec for the rod membranes (C).

plotted against time after a light flash. From the initial slope, the rate of total phosphorylation was calculated and was plotted against bleach level (Figure 6B and C). In the cone membranes (Figure 6B), the total phosphorylation rate increased as the bleach level increased. In contrast, in the rod membranes (Figure 6C), the rate stayed at almost a constant level when the bleach level was >3.9%.

The result in Figure 6C suggested that in the rod membranes, rod kinase fully expresses its activity at 3.9% bleach and the total phosphorylation rate does not increase even when more rod pigment is bleached. In contrast, cone kinase seems to be able to phosphorylate bleached cone pigment at much higher bleach levels (Figure 6B). These results probably explain the long saturation in rod responses and quick recovery in cone responses at high bleach levels. For comparison, saturated photoresponses of carp red-sensitive cones at bleach level of 28% (Figure 6B inset) and those of frog rods at the bleach level of 0.3% (Figure 6C inset) are shown. The photoresponses of carp rods were rather small in amplitude (<2 pA), and reliable measurements were not possible.

Discussion

I showed the early time course of rapid visual phosphorylation in cones (Figure 5). This rapid phosphorylation in cones probably explains why cone photoresponses recover quickly and do not saturate under intense background light (Figure 6).

Comparison of time courses between pigment phosphorylation and photoresponse recovery

The study of the phototransduction mechanism has been performed mainly in rods, and it has been generally known that rod visual pigment phosphorylation measured biochemically is much slower than a rod photoresponse recovery. One of the problems present in this inconsistency is that the light intensity usually used in the phosphorylation measurement is > 10^3 times higher than that used in the photoresponse measurement so that both reactions cannot be compared directly. Because the light intensity required for generation of a photoresponse is much higher in cones, it may be possible to compare the time courses directly between pigment phosphorylation and photoresponse recovery in cones.

In Figure 5D inset, I showed that carp red-sensitive cone photoresponses elicited by a light flash of similar light intensity used in the phosphorylation measurement started to recover at 0.3 s after the flash. At the time of this recovery, about two phosphates were incorporated into an activated cone visual pigment. It is known that similar number of phosphates should be necessary for the complete suppression of the light-activated visual pigment in rods (Mendez *et al.*, 2000). Thus, the result showed that the time course of visual pigment phosphorylation coincides with the photoresponse recovery.

In intact photoreceptors, Ca^{2+} concentration decreases in light (Pugh and Lamb, 2000; Burns and Arshavsky, 2005; Fu and Yau, 2007), and this decrease would cause disinhibition of the visual pigment kinase activity through inactivation of S-modulin/visinin (Kawamura, 1993; Kawamura *et al.,* 1996; Dizhoor *et al.,* 1991). Because biochemical measurement in this study was done at a constant low Ca^{2+} concentration without the inhibition of visual pigment kinase by S-modulin/visinin, the time course measured in this study could be a little bit faster than that observed in intact cells. However, because the Ca^{2+} concentration decrease in cones is rapid (τ = 43 ms) (Sampath *et al.,* 1999), its effect on the phosphorylation would not be so large in the case of

cones.

Phosphorylation at high bleach levels

The result in Figure 7 suggested that in cone membranes, cone kinase seems to be able to phosphorylate cone pigment at much higher bleach levels. This result probably explains the quick recovery in cone responses at high bleach levels. Quick recovery in cone responses seems to have important roles during light adaptation. When a background light is given, both rods and cones are initially hyperpolarized and then stabilized at a certain level. When an increment stimulus is given at this point, both rods and cones are hyperpolarized. When a momentary decrease in background illumination is given instead, rods do not respond, but cones depolarize quickly. This difference in the response to a decrement stimulus is attributable to the difference in the speed of the recovery of a photoresponse. In addition, rods are saturated with bright background light, but cones are hardly saturated even under extremely bright background light. It is highly possible that very effective phosphorylation of visual pigment in cones is one of the important underlying mechanisms of the above kinds of behavior of cones.

Part 2. Comparison of Ca^{2+}-dependent regulation of GRK1 by S-modulin and GRK7 by visinin

Introduction

It is known that the activity of G-protein coupled receptor kinase (GRK; GRK1 in rods) is inhibited in a Ca^{2+}-dependent manner by a neuronal calcium sensor protein (NCS), S-modulin in frog (Kawamura and Murakami, 1991; Kawamura, 1993) or its bovine orthologue, recoverin (Dizhoor *et al.*, 1991; Kawamura *et al.*, 1993). Under dark-adapted conditions, the cytoplasmic Ca^{2+} concentration is high. When GRK1 becomes active under this condition, the Ca^{2+}-bound form of S-modulin/recoverin directly binds to GRK1 to inhibit its kinase activity (Figure 7, upper) (Gorodovikova and Philippov, 1993; Chen *et al.*, 1995; Sato and Kawamura, 1997). With this mechanism, S-modulin/recoverin prolongs the lifetime of activated visual pigment when the cell is stimulated by a light flash under dark-adapted conditions. In contrast, when the cell is light-adapted, cytoplasmic Ca^{2+} concentration is low. Under this condition, the Ca^{2+}-free form of S-modulin/recoverin does not inhibit GRK1 so that the lifetime of activated visual pigment becomes short (Figure 7, lower). Recent studies using recoverin knock-out mice support this view (Makino *et al.*, 2004; Sampath *et al.*, 2005).

The above studies were performed mainly in rods. In cone photoreceptors, as described in general introduction, similar phototransduction mechanism is known to be present, and a cone version of a phototransduction protein is found in many of the animals. Previous studies showed that a cone homologue of S-modulin/recoverin, visinin, is present in chicken (Yamagata *et al.*, 1990) and that frog visinin (Kawamura *et al.*, 1993) inhibits phosphorylation of light-activated rod visual pigment at high Ca^{2+} concentrations as S-modulin does (Kawamura *et al.*, 1996). However, the inhibition of cone visual pigment kinase, GRK7, by visinin has not been measured due to a difficulty in purification of cone photoreceptor cells in the amount sufficient to perform biochemical measurements. In the present study, by using purified carp rods and cones, I measured both the inhibition of GRK7 by visinin in cones and the inhibition of GRK1 by S-modulin in rods. I first measured the expression levels of S-modulin and visinin, and estimated their concentrations in the outer segment. I also compared the dose-dependency and the Ca^{2+} concentration-dependency of the

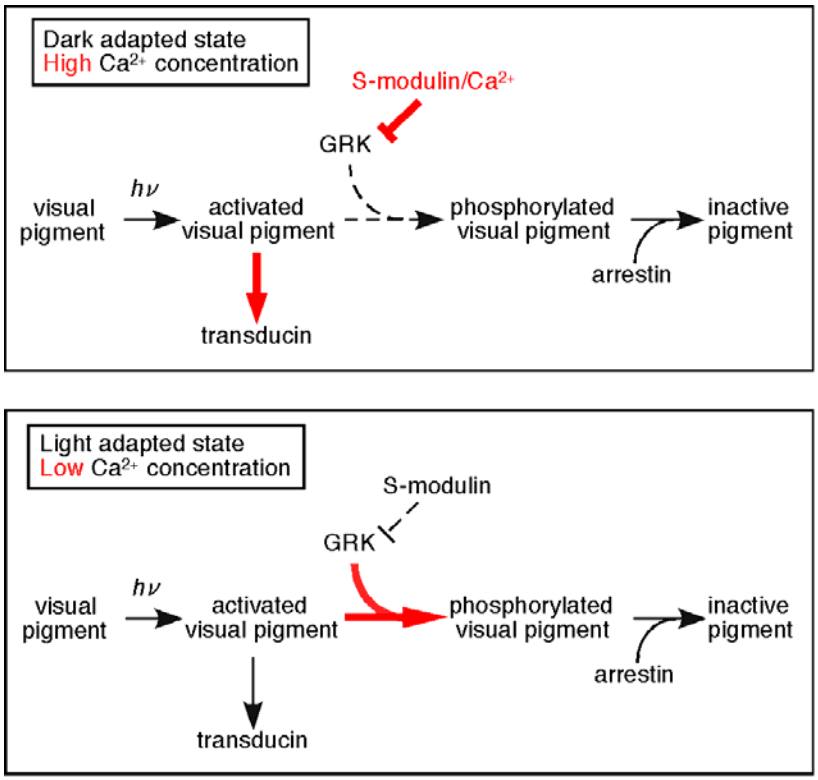

Figure 7. Scheme of visual pigment phosphorylation in dark-adapted and in light-adapted state. (*Top*) In dark-adapted state, the cytoplasmic Ca^{2+} concentration in a photoreceptor cell is in a range of several hundred nanomolar (McCarthy *et al.* (1996) and Sampath *et al.* (1998)). Under this condition, S-modulin binds Ca^{2+} and inhibits GRK activity. The inhibition of GRK by S-modulin can probably lengthen the lifetime of the activated visual pigment. (*Bottom*) In light-adapted state, the Ca^{2+} concentration decreases so that visual pigment phosphorylation is not inhibited by S-modulin. As a result, the lifetime of the activated visual pigment decreases.

inhibitory effect of S-modulin on GRK1 in rods and that of visinin on GRK7 in cones. The result showed that the maximum inhibition is higher in cones than in rods. However, although S-modulin and visinin exhibit <70% amino acid identity in carp, they showed very similar inhibition effects on GRK1 and GRK7.

In previous studies, it has been shown that the N-terminal region of GRK1 (Higgins *et al.*, 2006; Ames *et al.*, 2006) and that of GRK7 (Torisawa *et al.*, 2008) are the binding sites to the Ca^{2+}-bound form of S-modulin/recoverin. Then, to investigate why the inhibitory effect of visinin on

GRK7 in cones is higher than that of S-modulin on GRK1 in rods, I also compared the association and dissociation kinetics of the interaction of GRK1 with S-modulin in rods and those of GRK7 with visinin in cones by using N-terminal peptides of GRK1 and GRK7.

Experimental Procedures

Preparation of S-modulin-free rod membranes and visinin-free cone membranes

Rods and cones purified by a stepwise Percoll density gradient were washed with and subsequently suspended in a K-gluc buffer 1. To eliminate endogenous S-modulin from rod membranes and visinin from cone membranes completely, the cells were first freeze-thawed, and the thawed cells were centrifuged (100,000 × g for 20 min) to isolate the membrane fraction. The membranes were washed twice with an EGTA buffer (potassium gluconate buffer 2 (K-gluc buffer 2; 115 mM potassium gluconate, 2.5 mM KCl, 3 mM $MgCl_2$, 10 mM HEPES, 1 mM dithiothreitol, pH 7.5) supplemented with 5 mM EGTA), and then twice with the K-gluc buffer 2 to replace the buffer solution. An aliquot of the washed membranes was used to quantify the amount of visual pigment in the rod and the cone membranes. The washed membranes were stored in the dark at -80°C until use.

Expression and purification of carp S-modulin and visinin

Carp S-modulin and visinin were cloned by using a carp retinal cDNA library (Shimauchi-Matsukawa *et al.*, 2005), and the nucleotide sequences were determined (GenBank accession numbers: AB193289 for S-modulin and AB507711 for visinin). The amino acid identity between S-modulin and visinin in carp was 65.6%. The coding region of S-modulin and visinin were amplified from the carp retinal cDNA library by PCR with a pair of primers, each of which contained a site for a restriction enzyme. The sequences of the primers were: 5'-CATATGGGGAACACCAAGAG-3' (forward) and 5'-GGATCCTTAATGCTTCTTCT-3' (reverse) for S-modulin; 5'-CATATGGGGAATGCCAAAAG-3' (forward) and 5'-GGATCCTTATTTTTGGGGCT-3' (reverse) for visinin. The *Nde1*- and *BamH1*-digested cDNA was ligated with pET-3a (Novagen, Darmstadt, Germany). The recombinant plasmids were introduced into *Escherichia coli* BL21DE3 (Novagen) that was previously transformed with the vector of yeast N-myristoyl transferase (Duronio *et al.*, 1990). Recombinant myristoylated carp S-modulin and carp visinin were overproduced in *E.coli* and purified with a phenyl Sepharose column and a DEAE column as described previously (Kawamura *et al.*, 1996). After purification, samples were concentrated and the buffer solution of a sample was replaced with a K-gluc buffer 2.

Phosphorylation assays for measurement of inhibitory effect of S-modulin and visinin

Phosphorylation assay for measurement of inhibitory effect of S-modulin and visinin was performed as described above with some modifications. A reaction mixture was prepared by mixing 5 μL of S-modulin-free rod or visinin-free cone membrane suspension, 5 μL of an S-modulin or visinin solution of various concentrations and 5 μL of a high Ca^{2+}-concentration buffer (K-gluc buffer 2 supplemented with 3 mM $CaCl_2$) or a low Ca^{2+}-concentration buffer (K-gluc buffer 2 supplemented with 3 mM EGTA). To determine the maximum inhibition and minimum inhibition by S-modulin or visinin, the above extreme conditions (3 mM $CaCl_2$ or 3 mM EGTA) were used. An ATP solution (10 μL) containing 2.5 mM [γ-^{32}P] ATP and 1.25 mM GTP in K-gluc buffer 2 was added to the reaction mixture. The final concentrations of the components in a sample were 0.3 μM rod or cone visual pigment, up to 1 mM S-modulin or visinin, 3 mM $CaCl_2$ or 3 mM EGTA, 1 mM ATP and 0.5 mM GTP. When N-terminus peptides of GRK1 and GRK7 were used, they were dissolved firstly in dimethylsulfoxide and then used as reported previously (Torisawa *et al.*, 2008).

The bleach level of visual pigments was 75% in rod membranes and 95% in cone membranes. Then, the reaction in the rod membranes was terminated by adding the acid at 40 sec after the light flash, and the reaction in cone membranes was terminated at 0.5 sec after the light flash. In both cases, the reactions were terminated during the phase where the phosphorylation level increased linearly.

Immuno-quantification of endogenous S-modulin and visinin

Anti-S-modulin antiserum and anti-visinin antiserum were raised against bullfrog S-modulin and visinin, respectively, in a rabbit as reported previously (Kawamura *et al.*, 1993). To quantify the amounts of S-modulin and visinin expressed in carp rods and cones, respectively, immunoblot signal of S-modulin in purified rods and that of visinin in purified cones were compared with those obtained from known amounts of recombinant carp S-modulin and visinin. Purified rod and cone preparation were contaminated slightly (<2%) with cones and rods, respectively (Miyazono *et al.*, 2008). Although both of anti-S-modulin and anti-visinin antiserum cross-react to visinin and S-modulin, respectively, mobility of carp S-modulin on SDS-PAGE gel is lower than that of carp visinin as in the case of frogs (Kawamura *et al.*, 1996). Therefore, it was possible to quantify

S-modulin and visinin separately even in the present of contaminant.

Immunofluorescent staining of isolated photoreceptor cells

Carp rods and cones were isolated in the dark by using a Percoll density gradient similarly described above. However, in the study of immunofluorescent staining, rods and cones were purified simultaneously with a simplified method by using a stepwise Percoll density gradient consisted of only 30 and 90% Percoll in the present of 4% (w/v) paraformaldehyde. Rods and cones were obtained at the surface between 30 and 90% Percoll. They were collected and washed twice with and suspended in the carp Ringer's solution supplemented with 4% (w/v) paraformaldehyde. After the cells were kept at 4°C for 12 h for fixation in the dark, they were mounted on an aminopropylsilane-coated slideglass, and incubated for 15 min at room temperature to stick cells on the surface of a slideglass. Then, the slideglass was rinsed with a phosphate-buffered saline (PBS; 137 mM NaCl, 2.7 mM KCl, 8.1 mM Na_2HPO_4, 1.5 mM NaH_2PO_4, pH 7.4). Mounted rods were permeabilized with 0.05% (w/v) Triton X-100 in PBS and cones were permeabilized with 1% (w/v) Triton X-100 in PBS (Chang and Gilbert, 1997). After wash with PBS three times, rods and cones were air-dried overnight at room temperature. Then, to reduce non-specific adsorption of antiserum, rods and cones were incubated at 4°C for 1 h in PBS containing 0.01% (w/v) or 0.2% (w/v) Triton X-100, respectively, in the present of 1.5% (v/v) normal goat serum. After wash with PBS three times, rods were incubated overnight at 4°C with anti-frog S-modulin antiserum (1:500 dilution). Cones were also incubated overnight at 4°C with anti-frog visinin antiserum (1:500 dilution). Rods and cones were then washed with PBS and incubated at room temperature for 30 min with anti-rabbit IgG (Vector Laboratories, Burlingame, CA) conjugated with fluorescein isothiocyanate.

Calcium buffering

Solutions of different $CaCl_2$ concentrations and a fixed BAPTA concentration (1 mM BAPTA) in K-gluc buffer 2 were prepared. The free Ca^{2+} concentration in the solution was calibrated with Fluo-3 by using commercially available Ca^{2+}-concentration standard solutions (Calbuf-2; WPI, Sarasota, FL).

Peptides

A synthesized N-terminus peptide of carp GRK1A (2-29 aa) was obtained from GeneDesign (Ibaraki, Japan) and a synthesized N-terminus peptide of carp GRK7 (3-36 aa) was obtained from GenScript (Scotch Plains, NJ). The purity of a peptide was > 80%.

To conjugate these peptides to an IAsys cuvette (see below), an additional cysteine was introduced to the C-terminus of each of these peptides. There is a cysteine residue (Cys2) in the N-terminus of carp GRK7, but this cysteine residue was eliminated in the GRK7 peptide so that the GRK7 peptide was conjugated to the surface of the IAsys cuvette with its C-terminus.

S-modulin and visinin binding measurement

Ca^{2+}-dependent binding of S-modulin or visinin to the synthesized N-terminus peptide of GRK1 or GRK7 was monitored by a resonant mirror biosensor (IAsys; Affinity Sensors, Cambridge, UK) (Torisawa *et al.*, 2008). The N-terminus peptide of GRK1 or that of GRK7 was immobilized to carboxymethylated dextran (CMD) on the surface of an IAsys cuvette according to manufacturer's protocol. Succimide ester-activated CMD was conjugated to the thiol group of the C-terminus cysteine of the peptide through a linker, sulfosuccimidyl 4-(*N*-maleimidomethyl) cyclohexane-1-carboxylate (Pierce, Rockford, IL).

For the measurement of a Ca^{2+}-dependent binding of S-modulin or visinin to these peptides, I first added 75 μL of a low Ca^{2+}-HEPES buffer (10 mM HEPES, 120 mM KCl, 20 mM $MgCl_2$, 0.002% (w/v) Tween 80, 0.3 mM EGTA, pH 7.5) to the peptide-conjugated cuvette, and after stabilization of the resonance signal, I added 5 μL of S-modulin or visinin dissolved in the low Ca^{2+}-HEPES buffer to monitor the signal under the condition that no binding of S-modulin or visinin to the peptide was expected. On addition of S-modulin or visinin under this condition, the signal suddenly increased slightly most probably because of the increase in the refractive index induced by addition of S-modulin or visinin. Then, the signal was monitored for 3 min, and the signal stayed at almost a constant level during this period. The cuvette was then washed twice with the low Ca^{2+}-HEPES buffer to remove S-modulin or visinin. The cuvette was then equilibrated with 75 μL of a high Ca^{2+}-HEPES buffer (10 mM HEPES, 120 mM KCl, 20 mM $MgCl_2$, 0.002% (w/v) Tween 80, 0.3 mM $CaCl_2$, pH 7.5), and then 5 μL of S-modulin or visinin dissolved in the high Ca^{2+}-HEPES

buffer was added. Under high Ca^{2+} conditions, the signal increased significantly, most probably because of the binding of S-modulin or visinin to the peptide. Thus, I calculated the Ca^{2+}-dependent binding signal of S-modulin or visinin to the peptide by subtracting the signal observed under the low Ca^{2+} concentration from that observed under the high Ca^{2+} concentration. All measurements were performed at 25°C.

To determine the rate constants of association and dissociation of S-modulin to the GRK1 peptide, for example, I assumed a simple binding reaction:

$$S + P \underset{k_{off}}{\overset{k_{on}}{\rightleftharpoons}} SP \quad \cdots\cdots (1),$$

where S is the concentration of S-modulin, P is the concentration of the peptide, and k_{on} and k_{off} are the rate constants of association and dissociation, respectively. In this reaction, the rate of formation of SP is expected as:

$$d[SP]/dt = k_{on}[S][P] - k_{off}[SP] \quad \cdots\cdots (2).$$

Because [SP] + [P] is constant, i.e., equation (2) can be rearranged to:

$$d[SP]/dt = k_{on}[S][P_0] - [SP](k_{on}[S] + k_{off}) \quad \cdots\cdots (3).$$

I now assume that the concentration of unbound S-modulin ([S]) is approximately the same as the initial concentration of S ($[S_i]$), because only a small portion of S-modulin binds to the conjugated peptide. Then, equation (3) can be written as follows:

$$d[SP]/dt = k_{on}[S_i][P_0] - [SP](k_{on}[S_i] + k_{off}) \quad \cdots\cdots (4).$$

The value of [SP] is the amplitude of the signal. When the rate of rise of the signal (d[SP]/dt) is plotted against [SP], the slope indicates the value of $k_{on}[S_i] + k_{off}$. At a certain concentration of $[S_i]$, the slope, $k_{on}[S_i] + k_{off}$, was first determination, and then similar determinations were repeated at

various $[S_i]$. From the plot of the value of k_{on} $[S_i] + k_{off}$ against $[S_i]$ in the binding of S-modulin to the GRK1 peptide, k_{off} is determined from the intersection with the y-axis.

Results

Expression levels of S-modulin and visinin in the outer segment

In previous studies in frog rods and cones (Kawamura, S., 1993; Kawamura *et al.*, 1993), S-modulin and visinin were obtained in the soluble protein fraction at low Ca^{2+} concentrations. At high Ca^{2+} concentrations, they bound to membranes, but significant portion of these proteins were also obtained in the soluble protein fraction. During the course of the present study in carp, I realized that carp S-modulin and visinin bind to membranes more firmly than those in frogs. As shown in Figure 8, S-modulin probed by anti-S-modulin antibody (Figure 8A) and visinin probed by anti-visinin antibody (Figure 8B) were almost exclusively present in the membrane fraction (ppt) at a high (0.5 mM) Ca^{2+} concentration (high Ca^{2+}), while they were eluted with successive washes from the membranes under a low Ca^{2+} condition (low Ca^{2+}, sup). With this characteristic taken into account, I tried to determine the concentration of S-modulin in the rod OS and that of visinin in the cone OS.

Most of purified rods and cones retain a portion of inner segment (IS) (Shimauchi-Matsukawa *et al.*, 2008). For this reason, first I prepared a homogenate of rods and that of cones to determine the content of S-modulin and visinin, respectively, in the whole part of the cell (OS portion plus IS portion). By using anti-S-modulin and anti-visinin antiserum, homogenates of purified rods and cones together with known amounts of recombinant S-modulin and visinin were electrophoresed and immunoblotted (Figure 8C). Based on the calibration curve thus obtained, I quantified the amount of S-modulin in the rod homogenate and that of visinin in the cone homogenate (arrows in Figure 8D). The result showed that the content of S-modulin in the rod homogenate was 0.013 ± 0.004 ($n = 12$) per rod visual pigment, and that of visinin in the cone homogenate was 0.38 ± 0.13 ($n = 9$) per cone visual pigment. It has been known that S-modulin and visinin localized throughout the entire photoreceptor cell (Dizhoor *et al.*, 1991; Kawamura *et al.*, 1996; Strissel *et al.*, 2005). To estimate the expression level of S-modulin in the rod OS and that of visinin in the cone OS in the dark, I tried to determine the relative amounts of these proteins present in the OS portion with an immunofluorescent study in a isolated cell that was kept in the dark throughout.

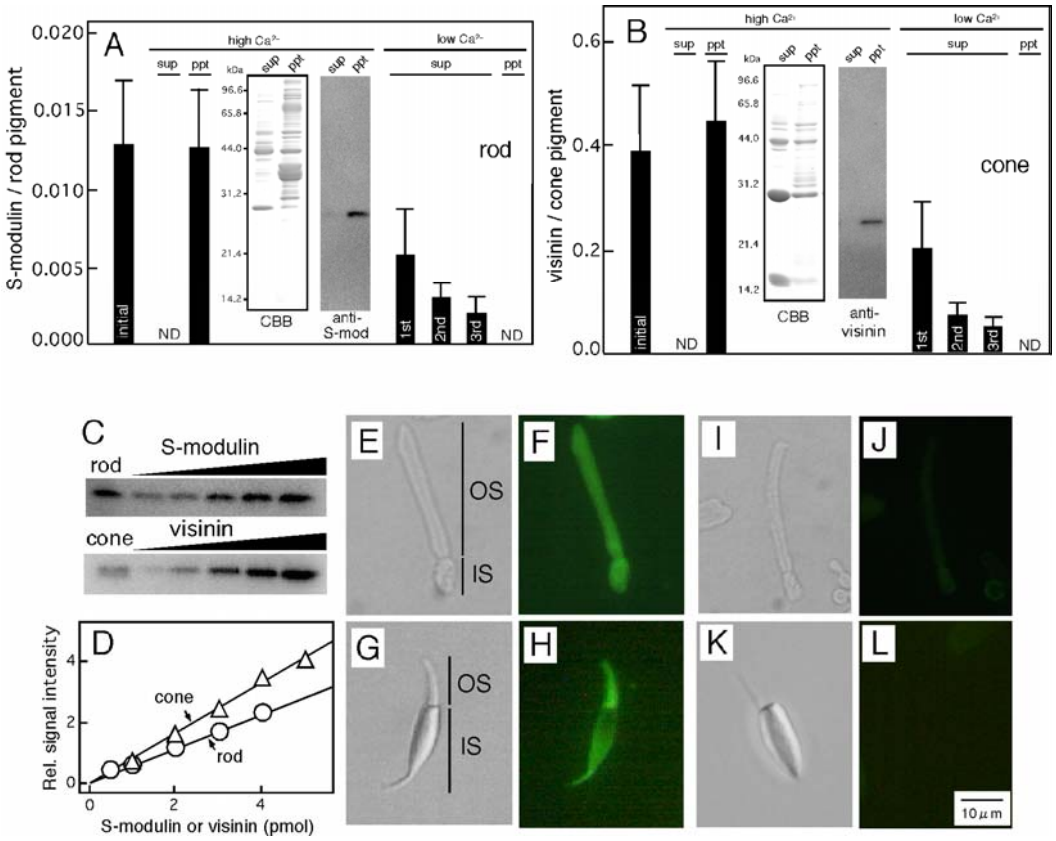

Figure 8. Expression levels of S-modulin and visinin in the OS of rods and cones. (A) Localization of S-modulin at high and low Ca^{2+} concentrations. The content of S-modulin was quantified in purified rods (*initial*). Rods containing 100 pmol of rod pigment prepared in the Ringer's solution at a high Ca^{2+} concentration (*high* Ca^{2+}) were homogenized and centrifuged. The contents of S-modulin in the soluble fraction (*sup*) and in the precipitated membrane fraction (*ppt*) were quantified. An example of immunoblot is shown in middle of the panel. Most of S-modulin was present in the membrane fraction (ND: not detected). Similarly, purified rods prepared in the K-gluc buffer 1 at a low Ca^{2+} concentration (*low* Ca^{2+}) were homogenized and centrifuged and the content of S-modulin in a soluble fraction (*sup*) was quantified (*1st*). The precipitate was suspended in the EGTA buffer and was centrifuged. The content of S-modulin in the soluble fraction was quantified (*2nd*). This procedure was repeated, and the content of S-modulin was quantified in the soluble fraction (*3rd*) and in the precipitated membrane fraction (*ppt*) (ND: not detected). (B) Similar as in (A) except that cone homogenate containing 5 pmol of cone pigment was used. (C) An example of quantification of S-modulin and visinin in rods and cones. The immunoblot signals were obtained in the samples of rod (upper panel) and cone (lower panel) homogenate. In addition, to obtain a calibration curve, known amounts of recombinant S-modulin (upper panel) and visinin (lower panel) were electrophoresed and immunoblotted. (D) Calibration curve obtained from quantification of the immunoblot signals in (C). The amount of S-modulin in rod homogenate and that of visinin in cone homogenate were determined (*arrows*). (E-H) Immunofluorescent staining of an isolated rod (E and F) and a cone (G and H). (I-L) Immunofluorescent staining of an isolated rod (I and J) and a cone (K and L) by normal mouse antiserum. E, G, I and K, phase contrast image of a rod (E and I) and a cone (G and K). F, H, J and L, immunofluorescent image of a rod (F and J) and a cone (H and L). *OS*, outer segment; *IS*, inner segment.

Immunofluorescent study showed that S-modulin in a rod (Figure 8F) and visinin in a cone (Figure 8H) distribute throughout the purified cell in agreement with previous studies. The intensity of the immunofluorescent signal in the OS relative to that in the whole part of the isolated cell was determined. The result showed that 68.1 ± 6.3% (n = 5) of S-modulin signal was localized in the OS of a purified rod, and 54.9 ± 8.2% (n = 8) of visinin signal was localized in the OS of a purified cone. Based on my determination of the content of S-modulin expressed in the unit of per visual pigment (see Figure 8A and B), the quantification of the fluorescent signal in the OS showed that the amount of S-modulin in the rod OS was 0.0088 (0.013 × 0.68) per rod pigment. Assuming that the overall visual pigment concentration is 3 mM in the OS and that the cytoplasmic volume of the OS is about a half of the OS volume, S-modulin concentration in the OS cytoplasm was calculated to be approximately 53 μM. This estimation is in good agreement with previous studies (see Discussion). The amount of visinin in the cone OS was 0.21 (0.38 × 0.55) per cone pigment, which corresponds to 1.2 mM under the same assumptions. The estimated concentration of visinin in the cone OS was found to be 20 times higher than that of S-modulin in the rod OS.

Comparison of inhibition of visual pigment kinase by S-modulin and visinin

Calcium ion-dependent inhibitory effect of S-modulin on rod visual pigment kinase, GRK1, was compared with that of visinin on cone visual pigment kinase, GRK7. Figure 9A shows the dose-dependent effect of S-modulin on the GRK1 activity in rod membranes at a low (open circles) and a high (filled circles) Ca^{2+} concentration. Figure 9B shows the results of similar studies of visinin on the GRK7 activity in cone membranes at a low (open triangles) and a high (filled triangles) Ca^{2+} concentration. To compare the inhibitory effect of S-modulin and visinin, the magnitude of the inhibition at the high Ca^{2+} concentration was calculated as the percentage of the maximum phosphorylation observed at the low Ca^{2+} concentration (Figure 9C). In both membranes, the inhibition on visual pigment kinase was progressively increased as the concentrations of S-modulin and visinin increased. The magnitude of the inhibition of GRK7 by visinin was slightly larger than that of GRK1 by S-modulin: visinin inhibited the GRK7 activity by 80% (filled triangles with thick solid line in Figure 9C) while S-modulin inhibited the GRK1 activity by less than 60% (filled circles with thick solid line). The half effective concentration (EC_{50}) of S-modulin on the

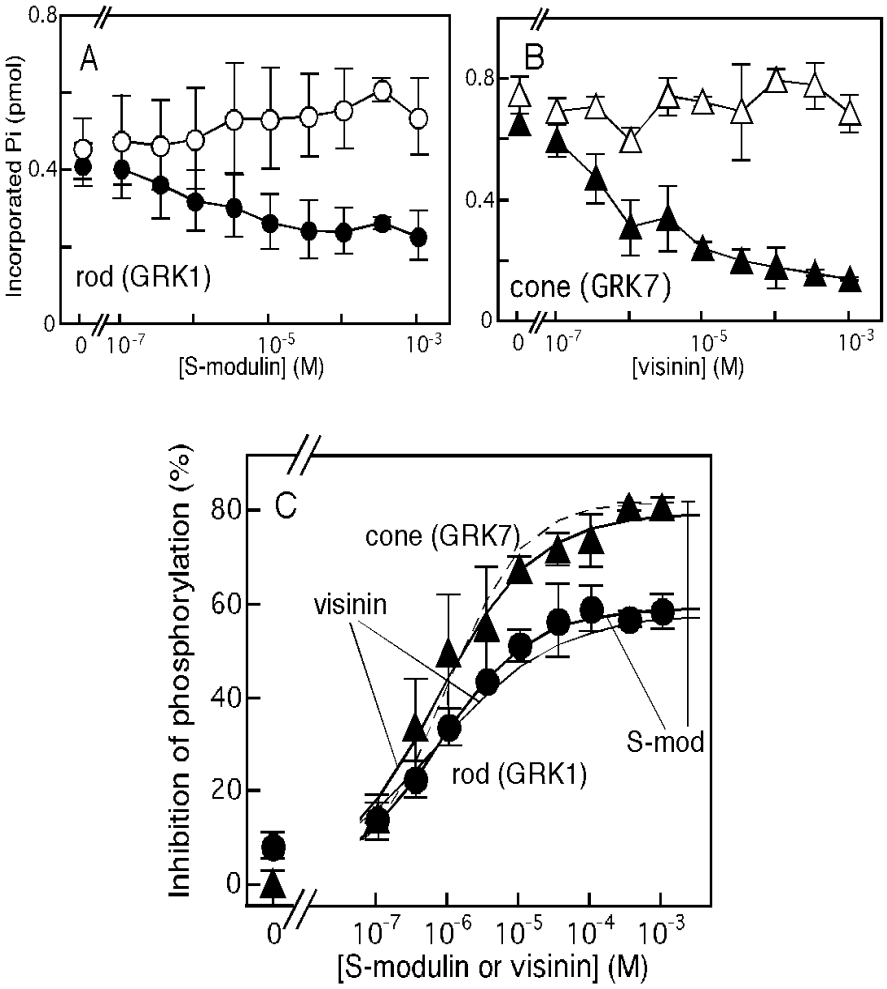

Figure 9. Concentration-dependent inhibition of visual pigment phosphorylation by S-modulin and visinin. (A) Phosphorylation of light-activated visual pigment was measured in rod membranes at various concentrations of recombinant S-modulin at a low (open circles) and a high (filled circles) Ca^{2+} concentration. (B) Similar as in (A), but the measurement was made in cone membranes with addition of various concentrations of recombinant visinin at a low (open triangles) and a high (filled triangles) Ca^{2+} concentration. (C) By taking the phosphorylation level at the low Ca^{2+} concentration to be 100% at each concentration of S-modulin or visinin, inhibition of the phosphorylation was calculated and shown as a function of S-modulin or visinin concentration. Inhibition of GRK1 by S-modulin (closed circles connected with thick solid line) and by visinin (thin solid line), and inhibition of GRK7 by visinin (closed triangles connected with thick solid line) and by S-modulin (thin dotted line) are shown. Result is shown as mean ± SD in three independent sets of measurement. Each curve in the panel shows the fitting by Michaelis-Menten equation with a Hill coefficient of 1.

GRK1 activity was 0.68 μM and that of visinin on the GRK7 activity was 0.67 μM.

It was of interest to know which of the two, visinin or GRK7, is responsible for the higher

inhibition of GRK7 by visinin. Therefore, the inhibition of GRK1 (rod GRK) by visinin (cone NCS) and the inhibition of GRK7 (cone GRK) by S-modulin (rod NCS) were measured. The result showed that visinin inhibited GRK1 activity only by 60% (thin solid line in Figure 9C) similarly as S-modulin did, and that S-modulin inhibited GRK7 activity by nearly 80% (thin dotted line) similarly as visinin did. To avoid crowdedness, only the lines connecting mean values are shown. In addition, half inhibition of a kinase, GRK1 or GRK7, was observed at very similar concentrations of visinin and S-modulin, respectively. It was evident from these measurements that higher inhibition in cones is attributed to the characteristic of GRK7 but not of visinin. Although S-modulin and visinin are expressed in a cell-type specific manner and their amino acid sequence identity is 66% in carp (see Experimental Procedures), they are functionally indistinguishable in terms of the effective concentrations of these proteins.

Effective ranges of Ca^{2+} concentration of S-modulin and visinin

To determine the difference in the Ca^{2+}-dependency of the regulation on GRK1 and GRK7 by S-modulin and visinin, the effective Ca^{2+} concentration range of S-modulin and that of visinin was compared. In Figure 10A, inhibition of GRK1 by 10 μM S-modulin (filled circles with thick line) and that of GRK7 by 10 μM visinin (filled triangles with thick line) were measured at various Ca^{2+} concentrations. Because S-modulin and visinin were used at 10 μM concentration, maximum inhibitions were slightly lower than those measured at the maximum doses in Figure 9C. Although the inhibition of GRK7 by visinin was higher than that of GRK1 by S-modulin (compared two thick lines) as was seen in Figure 9C, the EC_{50} values of the Ca^{2+}-effect were not different in these measurements. The values were 0.55 μM Ca^{2+} in the effect of S-modulin on GRK1 and 0.40 μM Ca^{2+} in the effect of visinin on GRK7.

I also measured the effect of Ca^{2+} on the inhibition of GRK1 (rod GRK) by visinin (cone NCS) and that of GRK7 (cone GRK) by S-modulin (rod NCS). As was seen in the measurement Figure 9C, S-modulin and visinin gave indistinguishable results: the EC_{50} value of Ca^{2+} concentration in the inhibition of GRK7 by S-modulin was 0.48 μM (thin dotted line) and that of GRK1 by visinin was 0.68 μM (thin solid line). In this measurement, it was confirmed that S-modulin and visinin are functionally indistinguishable.

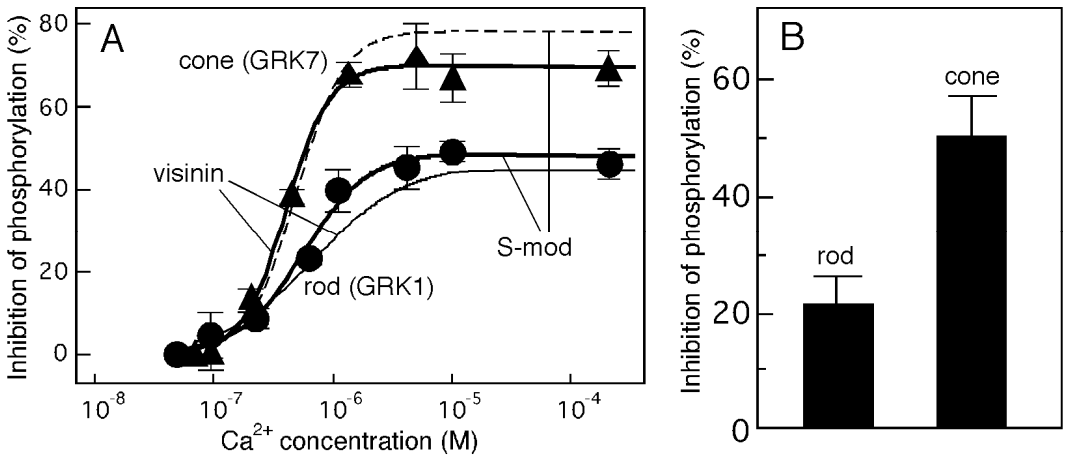

Figure 10. Effect of Ca^{2+} concentration on the inhibition of GRK activity by S-modulin and visinin. (A) Inhibition of pigment phosphorylation in rod or cone membranes by 10 μM S-modulin or 10 μM visinin is shown as a function of Ca^{2+} concentration. Inhibition was measured in a sample containing rod membranes and S-modulin (filled circles connected with thick solid line), rod membranes and visinin (thin solid line), cone membranes and S-modulin (thin dotted line), or cone membranes and visinin (filled triangles connected with thick solid line). Result is shown as mean ± SD in three independent sets of measurement. Each curve in the panel shows the fitting by Michaelis-Menten equation with a Hill coefficient of 1.6. (B) Inhibition of GRK activity by S-modulin and visinin under a pseudo-intracellular condition. GRK activity was measured in the presence of 53 μM S-modulin at 0.5 μM and 10 nM Ca^{2+} in rod membranes and in the presence of 1.2 mM visinin at 0.5 μM and 10 nM Ca^{2+} in cone membranes. The inhibition of phosphorylation at 0.5 μM Ca^{2+} was calculated based on the phosphorylation at 10 nM Ca^{2+} (n=3).

Estimation of the inhibition of GRK in the intact rod and cone OS

In the study shown in Figure 10A, the EC_{50} value of the Ca^{2+}-effect were 0.55 μM Ca^{2+} in rods (S-modulin and GRK1) and 0.4 μM Ca^{2+} in cones (visinin and GRK7). These concentrations are close to the level of Ca^{2+} concentration in the rod and cone OS in the dark (Sampath *et al.*, 1998; Sampath *et al.*, 1999), which indicates that the inhibition of GRK by S-modulin or visinin at the Ca^{2+} concentration in the dark is 50% or so. As shown in Figure 8, the concentration of visinin in the cone OS (1.2 mM) was much higher than the concentration of S-modulin in the rod OS (53 μM). To know the effect of these proteins in intact cells, inhibition of GRK1 by S-modulin and that of GRK7 by

visinin were measured under a pseudo-intracellular condition at the Ca^{2+} concentration in the dark, i. e., in the presence of 53 μM S-modulin at 500 nM Ca^{2+} in rod membranes and 1.2 mM visinin at 500 nM Ca^{2+} in cone membranes. The result showed that 21.7 ± 5.1% of GRK1 activity was inhibited in rod membranes and 53.2 ± 7.0% of GRK7 activity was inhibited in cone membranes (Figure 10B). It was, therefore, indicated that the inhibition by NCS would be 2.5 (53.2/21.7) times higher in cones than in rods at the Ca^{2+} concentration in the dark.

Inhibition of S-modulin and visinin by N-terminal peptides of GRK

As shown above, S-modulin and visinin showed very similar properties on the Ca^{2+}-dependent inhibition on the photoreceptor GRKs (Figure 9 and 10). In previous studies, it has been shown that the N-terminal region of rod kinase, GRK1 (Higgins *et al.*, 2006; Ames *et al.*, 2006) and that of cone kinase, GRK7 (Torisawa *et al.*, 2008) are the binding sites to the Ca^{2+}-bound form of S-modulin/recoverin. I then expected that an N-terminus peptide of GRK1 (most probably, competitively) inhibits S-modulin and visinin activities equally and that an N-terminus peptide of GRK7 inhibits S-modulin and visinin activities equally. However, because the inhibition of GRK7 by S-modulin and visinin was higher than that of GRK1 by these proteins (Figure 9 and 10), I expected further that the N-terminus peptide of GRK7 inhibits the S-modulin and visinin activities more effectively than the N-terminus peptide of GRK1.

I used an N-terminal peptide of GRK1 or GRK7 known to contain the region that inhibits the S-modulin/recoverin activity (Figure 11A). To measure the inhibitory effects of the peptides on S-modulin and visinin, the kinase could be either GRK1 or GRK7. For a practical reason, GRK1 was used in the following study. In the absence of S-modulin/visinin as control measurements, I first measured the effects of the N-terminus peptide of GRK1 to GRK1 activity. GRK1 activity was not affected by Ca^{2+} (left halves of Figure 11B and C). Addition of S-modulin (left half of Figure 11B) or visinin (left half of Figure11C) inhibited the phosphorylation at a high Ca^{2+} concentration to nearly 50% of the control in the absence of GRK1 peptide. Then the phosphorylation was measured in the presence of the GRK1 peptide of various concentrations and in the presence of either S-modulin (left half of Figure 11B) or visinin (left half of Figure11C). Addition of the GRK1 peptide in the absence of S-modulin or visinin reduced the phosphorylation in a Ca^{2+}-independent manner (left halves of

Figure 11B and C, and thick line in left half of Figure 11D).

To quantify the extent of the inhibition by the peptides, firstly the activity of S-modulin or visinin was defined (Torisawa *et al.,* 2008): the difference of the amounts of phosphorylation at a low and a high Ca^{2+} concentration in the absence of a peptide was divided by the amount of phosphorylation at the low Ca^{2+} concentration, and then this value was regarded as the 100% activity of S-modulin or visinin. After the activity of S-modulin or that of visinin in the presence of the peptide was calculated in a similar manner, the concentration-dependency of the peptide on the S-modulin and visinin activity was determined (thin and broken line, respectively, in left half of Figure 11D). Although the inhibition of the activities of S-modulin and visinin almost completed by 10 μM peptide, the inhibition of GRK1 by the peptide did not seem to be completed even at 0.5 mM peptide (see legend Figure 11D). This difference in the effective peptide concentrations indicated that the peptide affected the GRK1 activity and the S-modulin or visinin activity in different ways. It has been shown that the N-terminus region of GRK1 (17-34 aa) is also the binding site to R* (Palczewski *et al.,* 1993). Based on this finding, we speculated that the peptide bound to R* in addition to S-modulin and visinin, and inhibited their activities competitively. At the highest concentration of the peptide examined (0.5 mM), the GRK1 peptide inhibited the S-modulin activity to 44 ± 11% and the visinin activity to 37 ± 14% (left half of Figure11E). Similar measurements were carried out by using a GRK7 N-terminus peptide (right halves of Figure 11B, C and D). The inhibitions of S-modulin and visinin were higher when the GRK7 peptide was used: the GRK7 peptide inhibited the S-modulin activity to 30 ± 11% and the visinin activity to 21 ± 9%. The GRK1 peptide, and the GRK7 peptide, too, inhibited the S-modulin and the visinin activity to the same extent, but the inhibition was higher in the case of the GRK7 peptide as expected. One possibility to explain this result was that the N-terminus of GRK7 interacts more strongly to both S-modulin and visinin than the N-terminus of GRK1. The binding of the peptides to S-modulin and visinin was then directly measured.

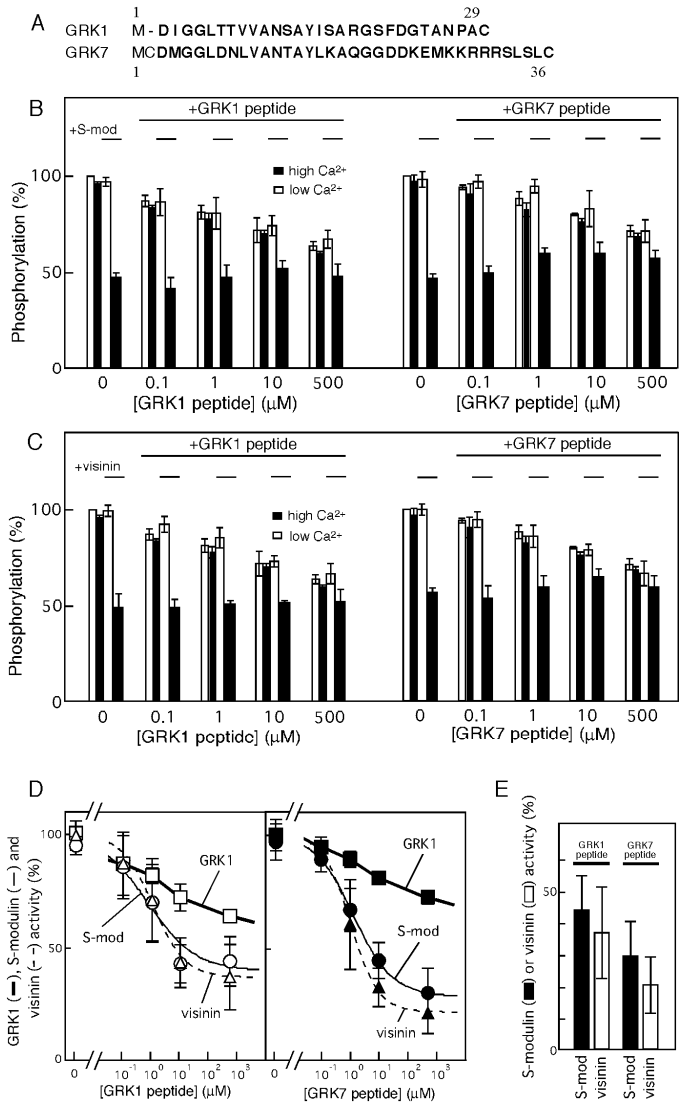

Figure 11. Inhibition of S-modulin and visinin by GRK N-terminus peptides. (A) N-terminus amino acid sequences of carp GRK1 and GRK7. Amino acid residues in the synthesized peptides are indicated in bold. In each peptide, a C-terminus cysteine residue was exogenously added (see Experimental Procedures). (B and C) Visual pigment phosphorylation was measured in rod membranes in the absence and presence of various concentrations of GRK1 N-terminus peptide or GRK7 N-terminus peptide in the absence and presence of 10 μM S-modulin (+S-mod; B) or 10 μM visinin (+visinin; C) at a low (open bars) and a high (filled bars) Ca^{2+} concentration. The phosphorylation level without addition of a peptide or S-modulin/visinin at the low Ca^{2+} concentration was set to 100%. (D) Activities of GRK1 at the low Ca^{2+} concentration in the absence of S-modulin or visinin (GRK1; thick line), S-modulin (S-mod; thin line) and visinin (visinin; broken line) are expressed against peptide concentration. Smooth line (S-modulin and visinin) was drawn according to Michaelis-Menten equation with a Hill coefficient of 1.0. Data points labeled as GRK1 did not fit to this equation so that they were connected with straight line. (E) Relative S-modulin and visinin activities in the presence of 0.5 mM peptide. Results shown are mean ± SD (n=3-6).

Binding of GRK1 and GRK7 peptide to S-modulin and visinin

The GRK1 peptide or the GRK7 peptide was immobilized on the carboxymethylated surface of an IAsys cuvette, and the Ca^{2+}-dependent binding of S-modulin and visinin to these peptides was monitored by a resonant mirror biosensor. Time courses of Ca^{2+}-dependent binding of S-modulin to the N-terminus of GRK1 peptide at various concentrations of S-modulin were measured (Figure 12A, upper panel). In a measurement at an S-modulin concentration of $[S_i]$, the value of k_{on} $[S_i]$ + k_{off} was determined (a circle shown in the lower panel of the Figure 12A; see Experimental Procedures) in the rising phase of the signal (indicated as "on" in Figure 12A), and it was plotted as a function of $[S_i]$ (association-dissociation plot; AD plot) (Figure 12A, lower panel). From this AD plot, the association rate constant (k_{on}) was determined from the slope and the dissociation rate constant (k_{off}) was determined from the intersection with the y-axis (see Experimental Procedures). Similar measurements and determinations were made in the binding of visinin to the GRK1 peptide (not shown), in the binding of S-modulin to the GRK7 peptide (not shown), in the binding of visinin to the GRK7 peptide (Figure 12B). Although some of the results are not shown, the AD plots of all of these measurements are summarized in Fig. 12C and D.

In Figure 12C, the binding of S-modulin to the GRK1 peptide is compared with that of visinin to the GRK7 peptide. It was found that association (compare the slopes) and dissociation (compare the y-axis) are both slightly faster in the binding of visinin to the GRK7 peptide than the binding of S-modulin to the GRK1peptide. In Figure 12D, the binding of S-modulin to the GRK7 peptide and that of visinin to the GRK1 peptide are compared. The determined rate constants (k_{on} and k_{off}) and the dissociation constant (K_D) calculated from the k_{off}/k_{on} value in each set of measurements are summarized in Table 1. It should be monitored here that the above measurements were done at high Ca^{2+} concentrations, and therefore, the rate constants and the dissociation constant are all those at high Ca^{2+} concentrations. There were slight differences in the association rate constant (k_{on}), the dissociation rate constant (k_{off}), and the dissociation constant (K_D) among each pair of NCS and GRK peptide. However, the K_D values of the GRK7 peptide in the binding to S-modulin and visinin were slightly lower (by 70-80%) than those of the GRK1 peptide (Table 1). This result was in agreement with my expectation that the GRK7 peptide interacts with S-modulin and visinin more strongly than the GRK1 peptide. In this table, the rate of dissociation constant determined in the dissociation phase

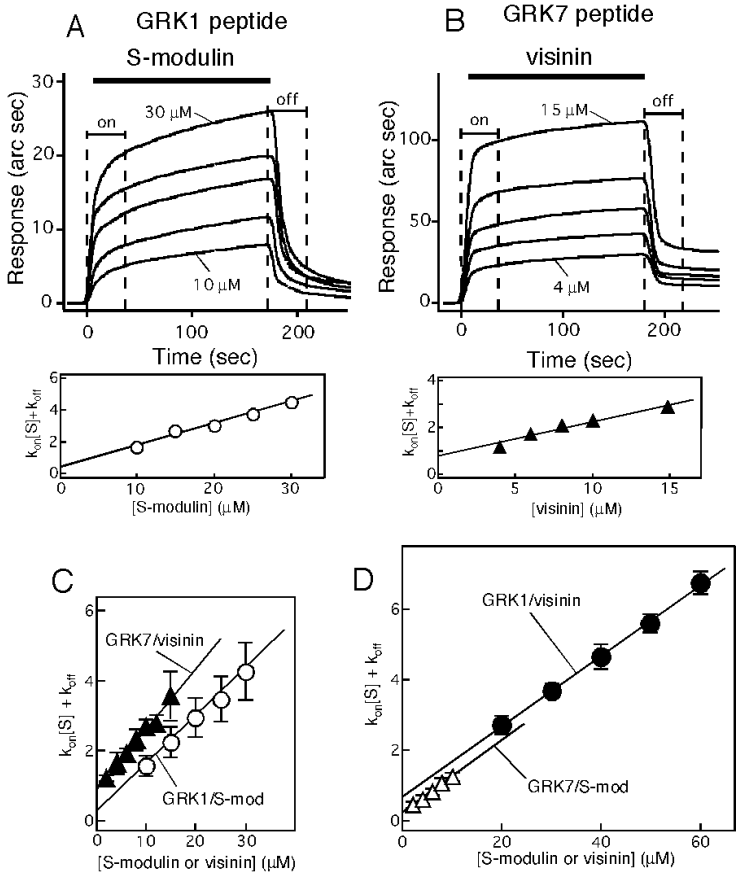

Figure 12. Binding of S-modulin and visinin to the N-terminal peptide of GRK. (A) Binding signals of S-modulin to an immobilized N-terminal peptide of GRK1 were monitored with a resonant mirror biosensor (upper panel). After addition of S-modulin at time 0, the signal increased because of Ca^{2+}-dependent binding of S-modulin to the immobilized peptide. At 3 minutes after the addition of S-modulin, S-modulin was washed out, and thus the binding signal decreased. The measurement was repeated by changing the concentration of S-modulin. From the rising phase of the signal (indicated as "on" in the upper panel), the value of k_{on} [S] + k_{off} at the S-modulin concentration of [S] was determined (see text), and it was plotted against the S-modulin concentration (lower panel; AD plot, see text). (B) Similar as in (A), but the measurement was made in the binding of visinin to a GRK7 N-terminus peptide. (C) AD plot of the binding of S-modulin to the GRK1 peptide (open circles) and that of visinin to the GRK7 peptide (filled triangles). (D) AD plot of the binding of visinin to the GRK1 peptide (filled circles) and that of S-modulin to the GRK7 peptide (open triangles).

of the reaction (indicated as "off" in Figure 12A, for example) is also shown (indicated as $*k_{off}$ in Table 1). The values were very similar to those determined in the analysis of an AD plot.

Table 1. Kinetic parameters of the binding of the N-terminal peptides of GRK1 and GRK7 to S-modulin and visinin.

	peptide	k_{on} (M^{-1} s^{-1})	k_{off} (s^{-1})	K_D (M)	*k_{off} (s^{-1})
S-modulin	GRK1	$1.3\pm0.3 \times 10^{5}$	$3.4\pm0.7 \times 10^{-1}$	$2.7\pm0.7 \times 10^{-6}$	$2.6\pm1.0 \times 10^{-1}$
	GRK7	$1.0\pm0.1 \times 10^{5}$	$2.3\pm0.7 \times 10^{-1}$	$2.2\pm0.7 \times 10^{-6}$	$2.9\pm0.2 \times 10^{-1}$
visinin	GRK1	$1.0\pm0.1 \times 10^{5}$	$7.1\pm1.1 \times 10^{-1}$	$7.1\pm1.1 \times 10^{-6}$	$6.9\pm2.6 \times 10^{-1}$
	GRK7	$1.7\pm0.2 \times 10^{5}$	$8.5\pm1.5 \times 10^{-1}$	$5.2\pm1.2 \times 10^{-6}$	$8.1\pm2.2 \times 10^{-1}$

The rate constants (k_{on} and k_{off}) were determined by analyzing the association phase of the IAsys signals shown in Fig. 12A-D. The dissociation constant (K_D) was calculated from k_{off}/k_{on}. The value of k_{off} was independently determined (*k_{off}) from the dissociation phase of the signals. Values are shown as mean ± SD (n=5-7).

Discussion

I showed that the estimated concentration of visinin in the cone OS was found to be 20 times higher than that of S-modulin in the rod OS (Figure 8). However, S-modulin and visinin are functionally indistinguishable (Figure 9 and 10A). The inhibition of GRK7 by visinin in cones would be 2.5 times higher than that of GRK1 by S-modulin in rods at the Ca^{2+} concentration in the dark (Figure 10B). I further demonstrated that GRK7 N-terminus peptide inhibited the S-modulin and visinin activity (Figure 11), and interacted with S-modulin and visinin more effectively than the GRK1 peptide (Figure 12 and Table 1).

Higher expression levels of NCSs over GRKs in rods and cones

In the present study, I estimated concentration of S-modulin in the rod OS and that of visinin in the cone OS (Figure 8). The estimated concentration of S-modulin in the carp rod OS was 53 μM, which was broadly in agreement with previous estimation of the S-modulin concentration in the frog rod OS (40 μM and 140 μM in Kawamura *et al.,* 1993 and Kawamura *et al.,* 1996, respectively). The visinin concentration in the carp cone OS (1.2 mM) was surprisingly higher when compared with that of S-modulin in the rod OS. In frogs, similar high expression level of visinin was actually observed: the molar ratio of S-modulin to visinin in a frog retina was found to be 10:7 even though the content of cone pigments was only 2% of that of rod pigment (Kawamura *et al.,* 1993). It should be emphasized that, based on the following calculation, the expression levels of S-modulin in rods and visinin in cones are much higher than those of GRKs in rods and cones. The GRK/visual pigment ratio is higher in cones than in rods (Tachibanaki *et al.,* 2005; Wada *et al.,* 2006) and that the ratios were 0.004 in rods and 0.04 in cones (Tachibanaki *et al.,* 2005). In my present study, I showed that S-modulin/visual pigment and visinin/visual pigment ratios in the OS were 0.0088 and 0.21, respectively (Figure 8). Therefore, S-modulin is present in the OS approximately 2 times more in amount than GRK1 (0.0088/0.004), and visinin is 5 times more than GRK7 (0.21/0.04). This higher ratio of NCS/GRK in cones would contribute to more effective inhibition of GRK in cones than in rods in intact cells.

Regulation of GRK activity in rods and cones

The maximal GRK7 activity in cones was ~0.4 phosphates incorporated per cone pigment present per sec (Pi/pigment-s) based on Fig. 6B. Let me assume that a very bright light is given in the dark and that GRK is activated fully. Just after this light stimulus, cytoplasmic Ca^{2+} concentration would still be high so that the activated GRK7 activity is inhibited by 53% (Figure 10B). When the Ca^{2+} concentration decreases during light-adaptation, GRK7 activity would increase from 0.2 (0.4 × 0.53) to 0.4 Pi/pigment-s. Similar calculation shows that the maximal GRK1 activity in rods was ~0.0053 Pi/pigment-s (Figure 6C). Thus, GRK1 activity increases from 0.0012 (22% inhibition of 0.0053 Pi/pigment-s at the Ca^{2+} concentration in the dark, Figure 10) to 0.0053 Pi/pigment-s during light-adaptation. Therefore, the actual range of regulation on GRK7 activity in cones (0.2 Pi/pigment-s) is much wider than the range of regulation on GRK1 activity in rods (0.004 Pi/pigment-s). This wide range of regulation on GRK7 would contribute to the wide range of regulation of cone light responses during light-adaptation.

Significance of cell-type specific expression of S-modulin and visinin

As reported previously in frogs (Kawamura *et al.,* 1996), rods and cones express different subtypes of NCS. The amino acid sequence analysis showed that S-modulin and visinin are 67% identical in frogs (Kawamura *et al.,* 1996) and 66% identical in carp (see Experimental Procedures). In the present study, I compared the dose dependency and the effective Ca^{2+} concentrations of the S-modulin and the visinin effects on GRK1 and GRK7 activities (Figure 9 and 10). The results showed that S-modulin and visinin were functionally indistinguishable. Although there is a cell-type specific expression of S-modulin and visinin in carp photoreceptors, I could not find any simple explanations why carp rods and cones have different subtype of NCS. This finding would be the indication that cell-type specific expression of a protein does not always mean that the protein has a cell-type specific effect.

Effective Ca^{2+} concentration for S-modulin and visinin

In salamander rods, Ca^{2+} concentration decreases from 670 nM in the dark to 30 nM in the light (Sampath *et al.,* 1998), and in salamander red-sensitive cones, it decreases from 410 nM in

the dark to 5.5 nM in the light (Sampath *et al.,* 1999). With this Ca^{2+} concentration range, S-modulin and visinin inhibited the visual pigment phosphorylation in the present study (Figure 10). The EC_{50} values of the Ca^{2+} concentration determined in the present study (0.4-0.55 μM) were several times lower than the values reported by others (2-3 μM Ca^{2+}) (Chen *et al.,* 1995; Calvert *et al.,* 1995). Although the reason of this inconsistency is not known, it may be the case that in the reconstituted membrane system used in others' studies, the effective Ca^{2+} concentration was somehow higher than that determined in the native membranes used in my studies. The study using recoverin knock-out mice (Makino *et al.,* 2004; Sampath *et al.,* 2005) also supports the view that S-modulin/recoverin functions under physiological Ca^{2+} concentrations.

Interaction between photoreceptor NCSs and GRK N-terminus peptides

In previous studies, the kinetics between recoverin and GRK1 were reported (Levay *et al.,* 1998; Satpaev *et al.,* 1998). In these studies, the association rate constant (k_{on}) and the dissociation constant (k_{off}) were 1.0×10^5 M^{-1} s^{-1} and 1.0×10^{-1} s^{-1}, respectively. The N-terminus region of GRK1 is thought to form an amphipathic helix, and the hydrophobic side of this helix is thought to bind to S-modulin/visinin (Higgins *et al.,* 2006; Ames *et al.,* 2006) at the groove in S-modulin/visinin formed by binding of Ca^{2+} (Tachibanaki *et al.,* 2000). In the present study, although I used only the N-terminus peptide, I obtained very similar values for the binding of S-modulin to GRK1 ($k_{on} = 1.3 \times 10^5$ M^{-1} s^{-1} and $k_{off} = 3.4 \times 10^{-1}$ s^{-1}; Table 1). The result strongly suggests that the binding of S-modulin/recoverin to GRK1 is mainly mediated by the interaction between S-modulin/recoverin and the N-terminus of GRK1. Although association and dissociation rate constants are similar in the binding of GRK1 whole protein and its N-terminus peptide to S-modulin/recoverin, the K_D value of the GRK1 peptide (2.7 μM, Table 1) is slightly higher than that of the GRK1 whole protein (approximately 0.7 μM, Figure 9). Because the association rate constant of the GRK1 peptide in the present study (1.3×10^5 M^{-1} s^{-1}) is very similar to that of the whole protein (1.0×10^5 M^{-1} s^{-1}), a slightly higher K_D value in the peptide is probably because of faster dissociation of the peptide (3.4×10^{-1} s^{-1}) than the whole protein (1.0×10^{-1} s^{-1}). Faster dissociation could be because the peptide may not be always in an ordered structure so that it could stay less stably in the binding site. The rates of association and dissociation are significantly higher than those measured in other reactions such as

the interaction between transducin $\beta\tilde{\gamma}$subunit and phosducin ($k_{on} = 3.8 \times 10^3$ M^{-1} s^{-1} and $k_{off} = 3.2 \times 10^{-4}$ s^{-1}) (Xu *et al.,* 1995) and that between transducin $\tilde{\alpha}$subunit and PDE $\tilde{\gamma}$subunit ($k_{on} = 7.9 \times 10^4$ M^{-1} s^{-1} and $k_{off} = 2.6 \times 10^{-3}$ s^{-1}) (Slepak *et al.,* 1995).

Part 3. Autophosphorylation of GRK1 and GRK7

Introduction

Similarly as other rod proteins in phototransduction cascade, the properties of GRK1 molecule have been investigated well. Analysis of the primary sequence of bovine GRK1 reveals that the kinase catalytic domain is located in the middle region of the sequence (Lorenz *et al*. 1991). The N-terminus of bovine GRK1 contains a domain participating in the recognition of activated visual pigment (Palczewski *et al*. 1993). Additionally, bovine GRK1 is modified by multiple intramolecular phosphorylations at the C and N termini of the enzyme (Palczewski *et al*. 1992). It has been shown that autophosphorylated bovine GRK1 lowers the affinity to S-modulin/recoverin (Satpaev *et al*., 1998). In contrast, only a few studies have reported the properties of cone GRK, GRK7 (Tachibanaki *et al*. 2005; Wada *et al*. 2006; Osawa *et al*. 2008). In these studies (Tachibanaki *et al*. 2005; Wada *et al*. 2006), it was shown that GRK7 has much higher kinase activity than GRK1 and its higher activity contributes to rapid turn-off of a photoresponse in a cone. It was of interest to examine whether this high GRK7 activity and the interaction with visinin are modulated by GRK7 autophosphorylation. For this purpose, I focused on autophosphorylation of GRK1 and GRK7. By using carp GRK1 and GRK7, I observed GRK1 and GRK7 autophosphorylation and measured their binding to S-modulin and visinin.

Experimental Procedures

Expression and purification of recombinant GRK1 and GRK7

Recombinant carp GRK1 and GRK7 were expressed in Sf9 cells and purified based on the method described previously (Chen *et al.*, 1995). Briefly, harvested cells were suspended and sonicated in a HEPES buffer (10 mM HEPES, 115 mM K-g potassium gluconate, 2.5 mM KCl, 2 mM $MgCl_2$, 1 mM dithiothreitol, pH 7.5) supplemented with 1 mM $CaCl_2$. The lysate was centrifuged (27,000 × g for 20 min), and the supernatant containing the kinase was collected. The kinases were affinity-purified with nonacylated S-modulin as described in Tachibanaki *et al.* (2000) and concentrated in K-gluc buffer 2. The amount of the expressed protein was quantified with Coomassie brilliant blue staining after SDS-PAGE, using BSA as a standard.

Immunoblot analysis of autophosphorylated GRK1 and GRK7

As reported previously (Tachibanaki *et al.*, 2005), anti-GRK1 antisera were raised against the C-terminus of (409-563 aa) of carp GRK1 in a mouse. Anti-GRK7 antisera were raised against a partial peptide of carp GRK7 (TGLFDELNDPNRKE, corresponding to the sequence at 519-532 aa) in a rabbit. Anti-GRK7 antibodies were affinity-purified with the GRK7 peptide.

To measure the autophosphorylation of GRK1 and GRK7, 10 μL of 2 mM ATP in K-gluc buffer 1 was mixed with 10 μL of 0.1 μM purified recombinant GRK1 or GRK7. After incubation for 40 min at room temperature, the reaction was terminated by adding 150 μL of 10% (w/v) trichloroacetic acid. After centrifugation (20,000 × g for 10 min), the precipitate was washed with K-gluc buffer 1 and subjected to SDS-PAGE, and GRK1 and GRK7 were immunoblotted by anti-GRK1 antisera and anti-GRK7 antisera, respectively. When GRK1 and GRK7 undergo autophosphorylation, each band of GRK1 and GRK7 detected with anti-GRK1 antisera and anti-GRK7 antisera, respectively, could be found at larger molecular weight because of incorporation of phosphates into GRK1 and GRK7.

Quantification of GRK1 and GRK7 autophosphorylation

Known amounts of purified recombinant GRK1 or GRK7 (5 pmol) were incubated with 1

mM [γ-^{32}P] ATP in K-gluc buffer 1 at 25°C. At various incubation times, reactions were terminated by mixing with 150 μL of 10% (w/v) trichloroacetic acid. After centrifugation (20,000 × g for 10 min), the precipitate was washed with K-gluc buffer 1 and subjected to SDS-PAGE, and the amount of ^{32}P incorporated into the GRK1 or GRK7 band was quantified by using an image analyzer (BAS 2500; Fuji Film, Tokyo, Japan).

Binding measurement of GRK1 to S-modulin and GRK7 to visinin

Ca^{2+}-dependent binding of GRK1 or phosphorylated GRK1 to S-modulin and that of GRK7 or phosphorylated GRK7 were monitored by IAsys. As has been used in the conjugation of recoverin to CMD (Satpaev *et al.*, 1998; Levay *et al.*, 1998), S-modulin was linked to CMD in an IAsys cuvette through the cysteine residue at the amino acid position of 39 (C39), the only cysteine residue in S-modulin. Although C39 is the only cysteine residue in S-modulin, there are two cysteine residues in carp visinin. The 3D structure of recoverin indicates that C39 is exposed to the surface of the molecule and that V126, which is replaced by C126 in carp visinin, is also present at the surface, although the latter seems to be surrounded by other residues. It is possible that either of the two cysteine residues was linked to CMD in my present study, but both C39 and V126 (C126 in carp visinin) are located at the opposite side of the molecule with respect to the reported binding site of S-modulin/recoverin to GRK1 (Tachibanaki, *et al.*, 2000). For this reason, I believe that the linkage by the linker molecule probably does not affect the binding of GRK7 to the binding site in a visinin molecule.

I measured a Ca^{2+}-dependent binding of GRK1 or phosphorylated GRK1 to S-modulin and that of GRK7 or phosphorylated GRK7 to visinin. Purified recombinant GRK1 or GRK7 was added to the cuvette at a high or a low Ca^{2+} concentration (0.3 mM $CaCl_2$ and 0.3 mM EGTA, respectively) to monitor the binding of GRK1 to S-modulin or that of GRK7 to visinin. When phosphorylated GRK1 or GRK7 was used 0.1 mM ATP was added to the cuvette.

Results

Autophosphorylation of GRK1 and GRK7 in vitro

Previous studies showed that bovine GRK1 undergoes autophosphorylation in an intramolecular reaction (Buczylko *et al.* 1991; Palczewski *et al.* 1992; Palczewski *et al.* 1995). It was indicated that there are three autophosphorylation sites in bovine GRK1. In comparison with bovine GRK1 amino acid sequence alignment, there are three potential autophosphorylation sites in carp GRK1 and only one in carp GRK7 (Figure 13A). By using purified recombinant carp GRK1 and GRK7, I measured that carp GRK1 and GRK7 actually undergo autophosphorylation (Figure 13B). Purified recombinant GRK1 incubated without ATP was detected at 64 kDa (Figure 13B, -ATP). After incubation with ATP, the signal was up-shifted and detected at 67 kDa (Figure 13B, +ATP). When incubated additionally with protein phosphatase 2A (see legend in Figure 13), GRK1 signal was detected again at 64 kDa (Figure 13B, +PP2A). As shown in Figure 13B right panel, purified recombinant GRK7 was slightly up-shifted after incubation with ATP (from 61 kDa to 62 kDa). However, the mobility of GRK7 was less than that of GRK1. Thus, it is indicated that GRK1 and GRK7 can be autophosphorylated *in vitro*, and that GRK1 has autophosphorylation sites more than GRK7.

To determine how many phosphates are incorporated into GRK1 and GRK7 molecule, I measured the stoichiometry of GRK1 and GRK7 autophosphorylation by using [γ-^{32}P] ATP. Figure 13C shows the time course of GRK1 and GRK7 autophosphorylation. GRK1 autophosphorylation reaction had a stoichiometry of about 3 phosphates per GRK1. On the other hand, about one phosphate was incorporated into GRK7. As compared with bovine GRK1 amino acid sequence alignment, there could be three autophosphorylation sites in carp GRK1 and only one in GRK7.

Autophosphorylation of GRK1 in rod membranes and that of GRK7 in cone membranes

By using purified rod membranes and cone membranes, I observed the status of autophosphorylation of GRK1 and GRK7 in rod and cone membranes, respectively. After incubation for 40 min in the absence or in the presence of ATP in the dark, the status of autophosphorylation of GRK1 and that of GRK7 were measured (Figure 14). Similarly as in recombinant GRK1, GRK1

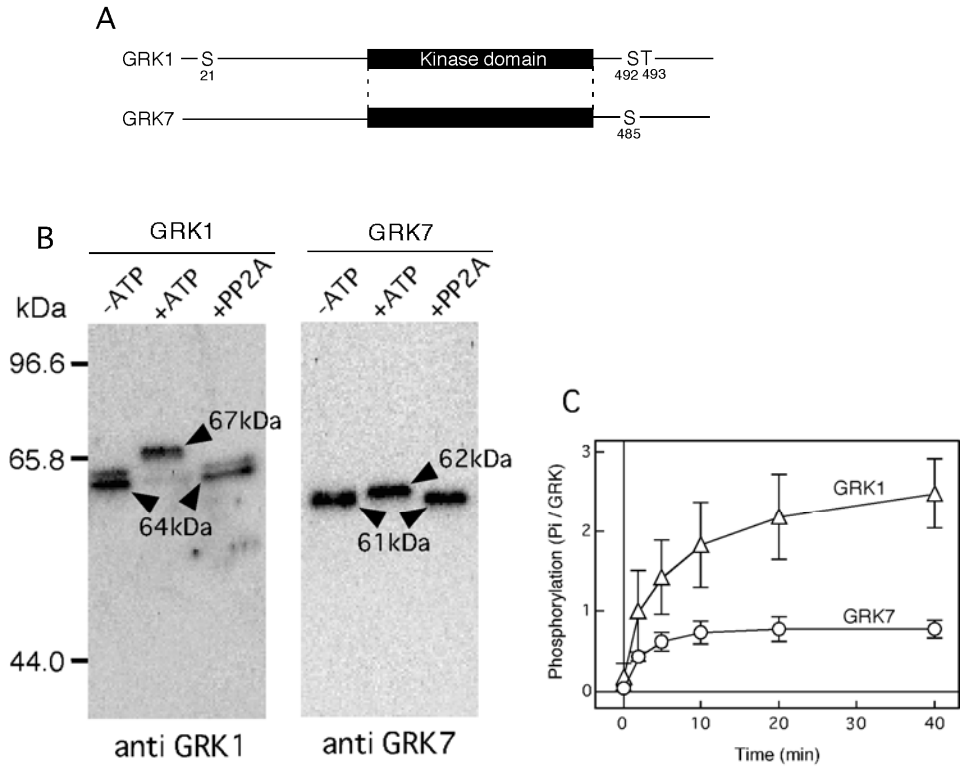

Figure 13. Autophosphorylation of recombinant GRK1 and GRK7. (A) Schematic diagrams of carp GRK1 and GRK7. Amino acid positions of the kinase domain (shown as thick bars) and potential amino acid residues for autophosphorylation (S or T) are indicated. (B) An example of immunoblot of recombinant GRK1 (left panel) and GRK7 (right panel) probed with anti-GRK1 antisera and anti-GRK7 antisera, respectively. (Left panel) Purified GRK1 incubated for 40 min in a K-gluc buffer 1 without ATP was detected at 64 kDa (-ATP). After incubation for 40 min in a K-gluc buffer 1 with ATP, GRK1 signal was detected at 67 kDa (+ATP). After the sample incubated with ATP was centrifuged (20,000 × g for 10 min), the precipitate was washed with K-gluc buffer 1 and incubated additionally with protein phosphatase 2A, PP2A, for 15 min. It is known that phosphorylated bovine GRK1 is a substrate for PP2A. When incubated with PP2A, GRK1 signal was detected again at 64 kDa (+PP2A). (Right panel) Similar as in left panel except that purified GRK7 was used. GRK7 signal was detected at 61 kDa (-ATP) and up-shifted slightly after incubation with ATP (+ATP). After incubated with PP2A, GRK7 signal was recovered at 61 kDa (+PP2A). (C) Time course of GRK1 (open triangles) and GRK7 (open circles) autophosphorylation (n = 3).

signal was detected at 64 kDa in the absence of ATP (Figure 14A, -ATP). The signal at 67 kDa was detected slightly. When incubated with ATP (Figure 14A, +ATP), the signal intensity at 67 kDa was increased (open arrow head in Figure 14A) and additional signals were detected between 64 kDa and 67 kDa band. It is probable that these are the bands of GRK1 in which one or two phosphates were

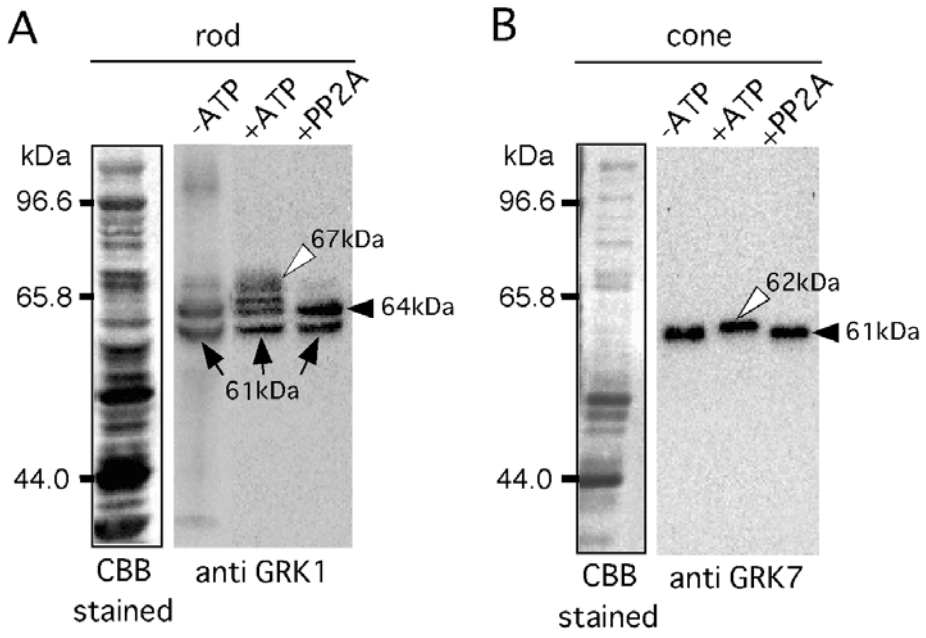

Figure 14. Autophosphorylation of GRK1 and GRK7 in purified rods and cones, respectively.

(A) An example of immunoblot of purified rod probed with anti-GRK1 antisera. Rods containing 250 pmol of rod pigment prepared in the K-gluc buffer 1 were used. Similarly as in recombinant GRK1 *in vitro*, GRK1 signal of purified rods was detected at 67 kDa (open arrow head) after incubation with ATP for 40 min in the dark (+ATP). When the sample was incubated with PP2A, the signal was recovered at 64 kDa (+PP2A, filled arrow head). 61 kDa signal was always detected even if the sample was incubated with ATP or PP2A (arrows). (B) Similar as in (A) except that purified cones containing 5 pmol of cone pigment were used.

incorporated because these bands were not detected after incubation with PP2A (Figure 14A, +PP2A). Therefore, GRK1 has ability of autophosphorylation in rod membranes. However, almost all of GRK1 molecule would not be phosphorylated in rod membranes in the dark because the signal of phosphorylated GRK1 at 67 kDa was not detected sufficiently (Figure 14A, -ATP). A signal at 61 kDa was always detected in purified rods, and the mobility did not change even when the sample was incubated with ATP or PP2A. It might be a non-specific signal.

Similar as in Figure 14A except that purified cones containing 5 pmol of cone pigment were used (Figure 14B). When cone membranes were incubated in the absence of ATP in the dark (Figure 14B, -ATP), phosphorylated GRK7 signal was not detected (compared -ATP with +ATP in Figure 14B). Therefore, GRK7 also would not be phosphorylated in cone membranes in the dark.

Binding of phosphorylated GRK1 to S-modulin and phosphorylated GRK7 to visinin

It has been reported that phosphorylated bovine GRK1 decreased GRK1-recoverin binding (Satpaev *et al.*, 1998). To investigate the binding of phosphorylated carp GRK1 to S-modulin, I measured the Ca^{2+}-dependent binding of unphosphorylated and phosphorylated carp GRK1 to S-modulin (Figure 15A). The response of phosphorylated GRK1 was slightly lower than that of unphosphorylated GRK1, but time courses of binding to S-modulin were almost the same (Figure 15A). It seems that there is no difference of binding to S-modulin in the presence or in the absence of autophosphorylation of GRK1. Similar results were obtained by using GRK7 (Figure 15B).

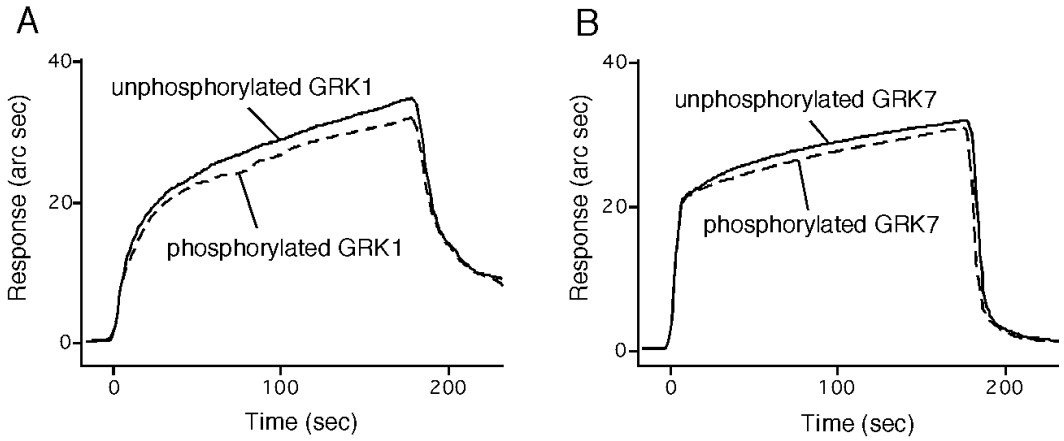

Figure 15. Binding of autophosphorylated GRK1 to S-modulin and autophosphorylated GRK7 to visinin. (A) Binding signal of unphosphorylated (thin line) and phosphorylated (broken line) GRK1 to an immobilized S-modulin were monitored with IAsys. After addition of GRK1 at time 0, the signal increased because of Ca^{2+}-dependent binding of GRK1 to the immobilized S-modulin. At 3 minutes after the addition of GRK1, GRK1 was washed out, and thus the binding signal decreased. The final concentration of GRK1 was 100 nM. (B) Similar as in (A), but the measurement was made in the binding of unphosphorylated (thin line) and phosphorylated (broken line) GRK7 to visinin.

Discussion

In the present study, I observed the autophosphorylation of GRK1 and GRK7 (Figure 13 and 14). The results showed that GRK1 and GRK7 can undergo autophosphorylation and GRK1 has multiple autophosphorylation sites. Although GRK1 and GRK7 have abilities to undergo autophosphorylation, they seem to be in unphosphorylated form in the membrane in the dark (Figure 14). I also measured the GRK1/GRK7 autophosphorylation not in the dark but in the light. However, phosphorylated GRK1 and GRK7 were not detected. I could not find light-dependent autophosphorylation of GRK1 and GRK7. It is interesting to know in what situation GRK1 and GRK7 undergo autophosphorylation under *in vivo* conditions.

I also compared the binding of unphosphorylated and phosphorylated GRK1 and GRK7 to S-modulin and visinin, respectively (Figure 15). Although I could not find any differences in the binding of unphosphorylated and phosphorylated GRKs to S-modulin/visinin, the association and the dissociation of GRK7 to visinin seem to be faster than those of GRK1 to S-modulin (compared the association and the dissociation phases in Figure 15A with those in Figure 15B). This fast association and dissociation in the binding of GRK7 to visinin is consistent with the results using GRK7 peptide (Table 1). GRK1/GRK7 bind to and phosphorylate activated visual pigments. Autophosphorylation of GRK may affect the binding of GRK to visual pigment.

Future perspectives

In the present study, I showed that GRK7 has much higher activity than GRK1 and suggested a significant contribution of GRK7 in the turn-off mechanism of a photoresponse in cones. I focused on the termination of photoresponse, especially inactivation of activated visual pigments. Additionally, it is thought that there are differences in inactivation processes of G protein, transducin, and cGMP phosphodiesterase (PDE) between rods and cones. If transducin and PDE remain in the active form even after activated visual pigments are inactivated, the photoresponse is not terminated. Therefore, it is thought that each activated enzyme in cone phototransduction cascade is inactivated faster than that in rod. It is necessary to examine the each inactivation process in detail for clarifying the difference of photoresponse between rods and cones.

In this study, I showed that the range of regulation on GRK7 by visinin in cones in a Ca^{2+}-dependent manner is wider than that on GRK1 by S-modulin in rods, and indicated that this wide range of regulation on GRK7 would contribute to the wide range of regulation of cone light responses during light adaptation. However, in spite of cell-type specific expression, S-modulin and visinin were functionally indistinguishable. This finding could be the indication that cell-type specific expression of a protein does not always mean that the protein has a cell-type specific effect. Actually, in some mammal cones, a cone specific protein is not present, or its rod type is expressed. Alternatively, S-modulin and visinin may have cell-type specific roles in the regulation of reaction other than visual pigment phosphorylation because S-modulin and visinin are distributed throughout rods and cones, respectively. It would be interesting to study the roles of S-modulin and visinin present in the cellular compartment other than the outer segment.

Like most protein kinases, GRK1 and GRK7 have abilities to undergo autophosphorylation. It has been reported that bovine phosphorylated GRK1 decreases the affinity to S-modulin/recoverin, but I could not find decrease of binding of carp phosphorylated GRKs to S-modulin/visinin. The role of autophosphorylation of GRK1/GRK7 has not been understood yet. Autophosphorylation of GRK may affect the binding of GRK to visual pigment. This point would be one of the future directions of the GRK1 and GRK7 study.

References

Ames, J. B., Levay, K., Wingard, J. N., Lusin, J. D. and Slepak, V. Z. (2006) Structural basis for calcium-induced inhibition of rhodopsin kinase by recoverin. *J. Biol. Chem.* **281,** 37237-37245.

Buczylko, J., Gutmann, C. and Palczewski, K. (1991) Regulation of rhodopsin kinase by autophosphorylation. *Proc. Natl. Acad. Sci. USA* **88,** 2568-2572

Burkhardt, D. A. (1994) Light adaptation and photopigment bleaching in cone photoreceptors in situ in the retina of the turtle. *J. Neurosci.* **14,** 1091-1105.

Burns, M. E. and Arshavsky, V. Y. (2005) Beyond counting photons: Trials and trends in vertebrate visual transduction. *Neuron* **48,** 387-401.

Calvert, P. D., Klenchin, V. A. and Bownds, M. D. (1995) Rhodopsin kinase inhibition by recoverin. *J. Biol. Chem.* **270,** 24127-24129.

Chang, H. and Gilbert, W. (1997) A novel zebrafish gene expressed specifically in the photoreceptor cells of the retina. *BiochemBiophys Res Commun.* **237,** 84-89.

Chen, C. K., Inglese, J., Lefkowitz, R. J. and Hurley, J. B. (1995) Ca^{2+}-dependent interaction of recoverin with rhodopsin kinase. *J. Biol. Chem.* **270,** 18060-18066.

Dizhoor, A. M., Ray, S., Kumar, S., Niemi, G., Spencer, M., Brolley, D., Walsh, K. A., Philipov, P. P., Hurley, J. B. and Stryer, L. (1991) Recoverin: A calcium sensitive activator of retinal rod guanylate cyclase. *Science* **251,** 915-918.

Duronio, R. J., Jackson-Machelski, E., Heuckeroth, R. O., Olins, P. O., Devine, C. S., Yonemoto, W., Slice, L. W., Taylor, S. S. and Gordon, J. I. (1990) Protein N-myristoylation in *Escherichia coli*: reconstitution of a eukaryotic protein modification in bacteria. *Proc. Natl. Acad. Sci. USA* **87,** 1506-1510.

Fain, G. L., Matthews, H. R., Cornwall, M. C. and Koutalos, Y. (2001) Adaptation in vertebrate photoreceptors. **81,** 117-151.

Fu, Y. and Yau, K.W. (2007) Phototransduction in mouse rods and cones. *Pflugers Arch.* **454,** 805-819.

Gorodovikova, E. N. and Philippov, P. P. (1993) The presence of a calcium-sensitive p26-containing

complex in bovine retina rod cells. *FEBS Lett.* **335,** 277-279.

Higgins, M. K., Oprian, D. D. and Schertler, G. F. (2006) Recoverin binds exclusively to amphipathic peptide at the N terminus of rhodopsin kinase, inhibiting rhodopsin phosphorylation without affecting catalytic activity of the kinase. *J. Biol. Chem.* **281,** 19426-19432.

Hisatomi, O., Matsuda, S., Satoh, T., Kotaka, S., Imanishi, Y. and Tokunaga, F. (1998) A novel subtype of G-protein-coupled receptor kinase, GRK7, in teleost cone photoreceptors. *FEBS Lett.* **424,** 159-164.

Kawamura, S. and Murakami, M. (1991) Calcium-dependent regulation of cyclic GMP phosphodiesterase by a protein from frog retinal rods. *Nature* **349,** 420-423.

Kawamura, S. (1993) Rhodopsin phosphorylation as a mechanism of cyclic GMP phosphodiesterase regulation by S-modulin. *Nature* **362,** 855-857.

Kawamura, S. and Tachibanaki, S. (2008) Rod and cone photoreceptors: Molecular basis of the difference in their physiology. *Comp. Biochem. Physiol.* **150**, 369-377.

Kawamura, S., Hisatomi, O., Kayada, S., Tokunaga, F. and Kuo, C.H. (1993) Recoverin has S-modulin activity in frog rods. *J. Biol. Chem.* **268,** 14579-14582.

Kawamura, S., Kuwata, O., Yamada, M., Matsuda, S., Hisatomi, O. and Tokunaga, F. (1996) Photoreceptor protein s26, a cone homologue of S-modulin in frog retina. *J. Biol. Chem.***271,** 21359-21364.

Kennedy, M. J., Dunn, F. A. and Hurley, J. B. (2004) Visual pigment phosphorylation but not transducin translocation can cntribute to light adaptation in zebrafish cones. *Neuron* **25,** 915-928.

Lamb, T. D. and Pugh, E. N. Jr. (2006) Phototransduction, dark adaptation, and rhodopsin regeneration. The proctor lecture. *Invet. Opthalmol. Vis. Sci.* **47,** 5137-5152.

Levay, K., Satpaev, D. K., Pronin, A. N., Benovic, J. L. and Slepak, V. Z. (1998) Localization of the sites for Ca^{2+}-binding proteins on G protein-coupled receptor kinase. *Biochemistry* **37,** 13650-13659.

Lorenz, W., Inglese, J., Palczewski, K., Onorato, J. J., Caron, M. G. and Lefkowitz, R. J. (1991) The receptor kinase family: primary structure of rhodopsin kinase reveals similarities to the

beta-adrenergic receptor kinase. *Proc. Natl. Acad. Sci. USA* **88**, 8715-8719.

Maeda, T., Imanishi, Y. and Palczewski, K. (2003) Rhodopsin phosphorylation: 30 years later. *Prog Retin Eye Res* **22,** 417-434.

Makino, C. L., Dodd, R. L., Chen, J., Burns, M. E., Roca, A., Simon, M. I. and Baylor, D. A. (2004) Recoverin regulates light-dependent phosphodiesterase activity in retinal rods. *J. Gen. Physiol.* **123,** 729-741.

McCarthy, S. T., Younger, J. P. and Owen, W. G. (1996) Dynamic, spatially nonuniform calcium regulation in frog rods exposed to light. *J. Neurophysiol.* **76**, 1991-2004.

Mendez, A., Burns, M. E., Roca, A., Lem, J., Wu, L. W., Simon, M. I., Baylor, D. A. and Chen, J. (2000) Rapid and reproducible deactivation of rhodopsin requires multiplephosphorylation sites. *Neuron* **28**, 153-164.

Miller, J. L. and Korenbrot, J. I. (1993) Phototransduction and adaptation in rods, single cones, and twin cones of the striped bass retina: Acomparative study. *Vis. Neurosci.* **10,** 653-667.

Miyazono, S., Shimauchi-Matsukawa, Y., Tachibanaki, S. and Kawamura, S. (2008) Highly efficient retinal metabolism in cones. *Proc. Natl. Acad. Sci. USA* **105**, 16051-16056.

Nakatani, K. and Yau, K. W. (1989) Sodium-dependent calcium extrusion and sensitivity regulation in retinal cones of the salamander. *J. Physiol. (London)* **409,** 525-548.

Normann, R. A. and Werblin, F. S. (1974) Control of retinal sensitivity. I. Light and dark adaptation of vertebrate rods and cones. *J. Gen. Physiol.* **63,** 37-61.

Osawa, S., Jo, R. and Weiss, E. R. (2008) Phosphorylation of GRK7 by PKA in cone photoreceptor cells is regulated by light. *J. Neurochem.* **107,** 1314-1324.

Palczewski, K., Buczylko, J., Hooser, P. V., Carr, S. A., Huddleston, M. J. and Crabb, J. W. (1992) Identification of the autophosphorylation sites in rhodopsin kinase. *J. Biol. Chem.* **267,** 18991-18998.

Palczewski, K., Buczylko, J., Lebioda, L., Crabb, J. W. and Polans, A. S. (1993) Identification of the N-terminal region in rhodopsin kinase involved in its interaction with rhodopsin. *J. Biol. Chem.* **268,** 6004-6013.

Palczewski, K., Ohguro, H., Premont, R. T. and Inglese, J. (1995) Rhodopsin kinase autophosphorylation. *J. Biol. Chem.* **270,** 15294-15298.

Pepperberg, D. R., Cornwall, M. C., Kahlert, M., Hofmann, K. P., Jin, J., Jones, G. J. and Ripps, H. (1992) Light-dependent delay in the falling phase of the retinal rod photoresponse. *Vis. Neurosci.* **8,** 9-18.

Perry, R. J. and McNaughton, P. A. (1991) Response properties of cones from the retina of the tiger salamander. *J. Physiol. (London)* **433,** 561-587.

Pugh, E. N., Jr. and Lamb, T. D. (2000) Phototransduction in vertebrate rods and cones; molecular mechanisms of amplification, recovery and light adaptation. *Handb. Biol. Phys.* **3,** 184-255.

Sampath, A. P., Matthews, H. R., Cornwall, M. C. and Fain, G. L. (1998) Bleached pigment produces a maintained decrease in outer segment Ca^{2+} in salamander rods. *J. Gen. Physiol.* **111,** 53-64.

Sampath, A. P., Matthews, H. R., Cornwall, M. C., Bandarchi, J. and Fain, G. L. (1999) Light-dependent changes in outer segment free-Ca^{2+} concentration in salamander cone. *J. Gen. Physiol.* **113,** 267-277.

Sampath, A. P., Strissel, K. J., Elias, R., Arshavsky, V. Y., McGinnis, J. F., Chen, J., Kawamura, S., Rieke, F. and Hurley, J. B. (2005) Recoverin improves rod-mediated vision by enhancing signal transmission in the mouse retina. *Neuron* **46,** 413-420.

Sato, N. and Kawamura, S. (1997) Molecular mechanism of S-modulin action: binding target and effect of ATP. *J. Biochem.* **122,** 1139-1145.

Satpaev, D. K., Chen, C. K., Scotti, A., Simon, M. I., Hurley, J. B. and Slepak, V. Z. (1998) Autophosphorylation and ADP regulate the Ca^{2+}-dependent interaction of recoverin with rhodopsin kinase. *Biochemistry* **37,** 10256-10262.

Shimauchi-Matsukawa, Y., Aman, Y., Tachibanaki, S. and Kawamura, S. (2005) Isolation and characterization of visual pigment kinase-related genes in carp retina: polyphyly in GRK1 subtypes, GRK1A and 1B. *Mol. Vis.* **11,** 1220-1228.

Shimauchi-Matsukawa, Y., Aman, Y., Tachibanaki, S. and Kawamura, S. (2008) Identification of differentially expressed genes in carp rods and cones. *Mol. Vis.* **14,** 358-369.

Slepak, V. Z., Artemyev, N. O., Zhu, Y., Dumke, C. L., Sabacan, L., Sondek, J., Hamm, H. E., Bownds, M. D. and Arshavsky, V. Y. (1995) An effector site that stimulates G-protein

GTPase in photoreceptors. *J. Biol. Chem.* **270,** 14319-14324.

Strissel, K. J., Lishko, P. V., Trieu, L. H., Kennedy, M. J., Hurley, J. B. and Arshavsky, V. Y. (2005) Recoverin undergoes light-dependent intracellular translocation in rod photoreceptors. *J. Biol. Chem.* **280,** 29250-29255.

Tachibanaki, S., Nanda, K., Sasaki, K., Ozaki, K. and Kawamura, S. (2000) Amino acid residues of S-modulin responsible for interaction with rhodopsin kinase. *J. Biol. Chem.* **275,** 24127-24129.

Tachibanaki, S., Tsushima, S. and Kawamura, S. (2001) Low amplification and fast visual pigment phosphorylation as mechanisms characterizing cone photoreceptors. *Proc. Natl. Acad. Sci. USA* **98**, 14044-14049.

Tachibanaki, S., Arinobu, D., Shimauchi-Matsukawa, Y. and Kawamura, S. (2005) Highly effective phosphorylation by G protein-coupled receptor kinase 7 of light-activated visual pigment in cones. *Proc. Natl. Acad. Sci. USA* **102**, 9329-9334.

Tachibanaki, S., Shimauchi-Matsukawa, Y., Arinobu, D. and Kawamura, S. (2007) Molecular mechanisms characterizing cone photoresponses. *Photochem. Photobiol.* **83**, 19-26.

Torisawa, A., Arinobu, D., Tachibanaki, S. and Kawamura, S. (2008) Amino acid residues in GRK1/GRK7 responsible for interaction with S-modulin/recoverin. *Photochem. Photobiol.* **84**, 823-830.

Wada, Y., Sugiyama, J., Okano, T. and Fukada, Y. (2006) GRK1 and GRK7: Unique cellular distribution and widely different activities of opsin phosphorylation in the zebrafish rods and cones. *J. Neurochem.* **98,** 824-837.

Weiss, E. R., Raman, D., Shirakawa, S., Ducceschi, M. H., Bertram, P. T., Wong, F., Kraft, T. W. and Osawa, S. (1998) The cloning of GRK7, a candidate cone opsin kinase, from cone- and rod-dominant mammalian retinas. *Mol. Vis.* **4,** 27.

Weiss, E. R., Ducceschi, M. H., Horner, T. J., Li, A., Craft, C. M. and Osawa, S. (2001) Species-specific differences in expression of G-protein-coupled receptor kinase (GRK)7 and GRK1 in mammalian cone photoreceptor cells: implications for cone cell phototransduction. *J. Neurosci.* **21,** 9175-9184.

Xu, J., Wu, D., Slepak, V. Z. and Simon, M. I. (1995) The N-terminus of phosducin is involved in

binding of βγsubunits of G protein. *Proc. Natl. Acad. Sci. USA* **92**, 2086-2090.

Yamagata, K., Goto, K, Kuo, C. H., Kondo, H. and Miki, N (1990) Visinin: a novel calcium binding protein expressed in retinal cone cells. *Neuron* **4,** 469-476.

A list of achievements

Shuji Tachibanaki, Daisuke Arinobu, Yoshie Shimauhi-Matshukawa, Sawae Tsushima, Satoru Kawamura (2005) Highly effective phosphorylation by G protein-coupled receptor kinase 7 of light-activated visual pigment in cones *Proc. Natl. Acad. Sci. USA* **102**, 9329-9334

Shuji Tachibanaki, Yoshie Shimauhi-Matshukawa, Daisuke Arinobu, Satoru Kawamura (2007) Molecular Mechanisms Characterizing Cone Photoresponses *Photochem. Photobiol.* **83**, 19-26

Aya Torisawa, Daisuke Arinobu, Shuji Tachibanaki, Satoru Kawamura (2008) Amino Acid Residues in GRK1/GRK7 Responsible for Interaction with S-Modulin/Recoverin *Photochem. Photobiol.* **84**, 823-830

Daisuke Arinobu, Shuji Tachibanaki, Satoru Kawamura
Higher inhibition of visual pigment kinase in cones than in rods by S-modulin and visinin 投稿中

第 74 回日本動物学会 2003. 9. 17-19
錐体における速い視物質リン酸化反応の分子メカニズム
有信大輔、橘木修志、津嶋佐和栄、松川淑恵、河村悟

第 8 回視覚科学フォーラム 2004. 7. 30-31
桿体と錐体の光応答形成における視物質リン酸化の寄与
有信大輔、橘木修志、津嶋佐和栄、松川淑恵、河村悟

第 75 回日本動物学会 2004. 9. 10-12
錐体におけるし物質リン酸化反応の特徴
有信大輔、橘木修志、河村悟

第 12 回日本光生物学協会年会　2005. 8. 5-7

錐体における速い視物質リン酸化反応とその調節機構

有信大輔、橘木修志、松川（嶋内）淑恵、河村悟

第 45 回日本生物物理学会年会　2007. 12. 21-23

Regulation of GRK1/GRK7 by S-modulin and s26

有信大輔、橘木修志、河村悟

第 46 回日本生物物理学会年会　2008. 12. 3-5

Regulation of GRK1/GRK7 by S-modulin/recoverin and s26

有信大輔、橘木修志、河村悟

Acknowledgements

I am grateful to Prof. Satoru Kawamura for invaluable discussions and suggestions through this study. Especially, electrophysiological recordings shown in Figure 5 and 6 were performed by Prof. Satoru Kawamura. I express gratitude to Prof. Satoru Kawamura again for this help. I am thankful to Dr. Shuji Tachibanaki for helpful discussions and advices. I thank Dr. Shuji Tachibanaki and Mr. Kimura for help in establishing the GRK expression system. I thank Prof. Akihiko Ogura, Prof. Seiki Kuramitsu and Prof. Kazuhiro Iwai for helpful discussion and critical reading of this thesis. Finally, I am indebted to all members of Kawamura laboratory for their useful discussions and supports.